

Projections of Physiologically Defined Subdivisions of the Inferior Colliculus in the Mustached Bat: Targets in the Medial Geniculate Body and Extrathalamic Nuclei

JEFFREY J. WENSTRUP, DAVID T. LARUE, AND JEFFERY A. WINER

Department of Neurobiology, Northeastern Ohio Universities College of Medicine, Rootstown, Ohio 44272-0095 (J.J.W.) and Division of Neurobiology, Department of Molecular and Cell Biology, University of California at Berkeley, Berkeley, California 94720-3200 (J.J.W., D.T.L., J.A.W.)

ABSTRACT

This study examined the output of the central nucleus of the inferior colliculus to the medial geniculate body and other parts of the nervous system in the mustached bat (*Pteronotus parnellii*). Small deposits of anterograde tracers (horseradish peroxidase, [³H]leucine, *Phaseolus vulgaris* leucoagglutinin, wheat germ agglutinin conjugated to horseradish peroxidase, or biocytin) were made at physiologically defined sites in the central nucleus representing major components of the bat's echolocation signal. The topography, frequency specificity, and axonal morphology of these outputs were studied.

The medial geniculate body was a major target of inferior collicular neurons, with three distinct input patterns. The projection to the ventral division was tonotopically organized, but had a relatively sparse contribution from neurons representing frequency modulated components of the biosonar pulse. The second input was to the rostral medial geniculate body, in which projections from inferior collicular neurons representing constant frequency sonar components were separated from those representing frequency modulated components. A third input was to the suprageniculate nucleus, which received strong, topographically arranged projections. Inputs to the dorsal nucleus and medial division were also observed.

Extrathalamic regions receiving input included the pontine gray, external nucleus of the inferior colliculus, pericolicular tegmentum, nucleus of the brachium of the inferior colliculus, and pretectum. These central nucleus projections differed in organization and the structure of axon terminals, suggesting different physiological influences on their target nuclei. These results demonstrate that the central nucleus has divergent projections to various sensory and premotor nuclei, besides its well-established projection to the medial geniculate body. © 1994 Wiley-Liss, Inc.

Key words: axons, auditory pathways, lateral lemniscus, pons, pretectum, *Pteronotus parnellii*

In the dark, at high speed, and often amid dense vegetation, the mustached bat (*Pteronotus parnellii*) navigates and catches insects by echolocation (Novick, 1963; Bateman and Vaughan, 1974). The bat relies on auditory cues to detect, locate, and identify prey and obstacles, coordinating its vocalization, locomotion, and other motor functions to capture the prey and avoid the obstacles. This demanding behavior entails rapid processing and extensive distribution of auditory information throughout the neuraxis. The inferior colliculus is a potential source of such a distribution since it integrates a wide range of inputs from lower auditory nuclei (Zook and Casseday, 1982b, 1987; Ross et al., 1988; Frisina et al., 1989). This paper describes its

outputs, i.e., the anatomical substrate of the distribution of information furnished by the inferior colliculus. What are the principal target nuclei of axons of the inferior colliculus, and how do the distribution and axonal morphology of inferior collicular inputs contribute to the functional and organizational properties in these target nuclei?

The major focus here is on the projection of the central nucleus of the inferior colliculus (ICC) to the medial

Accepted December 9, 1993.

Address reprint requests to Jeffrey J. Wenstrup, Department of Neurobiology, Northeastern Ohio Universities College of Medicine, 4209 St. Rt. 44, P.O. Box 95, Rootstown, OH 44272-0095.

geniculate body (MGB), which is the principal synaptic relay between the auditory midbrain and the cerebral cortex (Winer, 1992). In the mustached bat, significant changes in the complement and the organization of physiological responses occur between the ICC (Zook et al., 1985; O'Neill, 1985; Wenstrup et al., 1986; O'Neill et al., 1989) and auditory cortical fields (Suga and Jen, 1976; O'Neill and Suga, 1982; Suga et al., 1983; Suga, 1984), and some of these differences may arise within the MGB. If so, the tectothalamic projection occupies a pivotal role by reorganizing some ICC output to create new physiological response properties within MGB. For example, what distinguishes some cortical fields is their selectivity for combinations of spectrally distinct signal elements in the sonar pulse and echo (O'Neill and Suga, 1982; Suga et al., 1983; Suga and Horikawa, 1986); varieties of combination-sensitive neurons are sensitive to the frequencies of, or the delay between, the two elements. Cortical fields containing such neurons are topographically organized according to the frequencies or the timing of the signal combinations, and may represent relative velocity and distance of sonar targets, respectively (O'Neill and Suga, 1982; Suga et al., 1983; Suga, 1984). These physiological and organizational features appear to be absent from the inferior colliculus (O'Neill, 1985), but recent studies of the MGB have revealed both combination-sensitive responses as well as neurons that are sharply tuned and that respond well to tone bursts (Olsen, 1986; Olsen and Suga, 1991a,b). Do the projections of the tonotopically organized ICC provide the basis both for its tonotopic organization and for its combination sensitivity? The present study addresses this question by analyzing the projections of ICC frequency bands representing major components of the bat's echolocation signal.

The ICC projects to targets besides the medial geniculate body. While some targets are relatively consistent across

species, such as the external nucleus of the inferior colliculus (Moore et al., 1977; Andersen et al., 1980; Kudo and Niimi, 1980; Schweizer, 1981; Saldaña and Merchán, 1992), others are more variable. For example, projections to nuclei of the pontine gray seem to be absent in rats (Mihailoff et al., 1989), equivocal in cats (Andersen et al., 1980; Hashikawa, 1983; Aas, 1989), but prominent in bats (Schweizer, 1981; Frisina et al., 1989; Wenstrup, 1990; Schuller et al., 1991). This report considers the topography and frequency composition of these extrathalamic projections to advance our understanding of their role in the bat's sonar behavior.

Elsewhere in the auditory system, the structure and distribution of axons are known to play a central role in regulating the discharge properties of postsynaptic neurons, an outstanding example being the functional relationship between endbulbs of Held and the bushy cells of the anteroventral cochlear nucleus (Wu and Oertel, 1984; Smith and Rhode, 1987; Ryugo and Rouiller, 1988; Liberman, 1991; Ryugo and Sento, 1991). In the auditory thalamus and other ICC targets, the structure of axon terminals may likewise determine what effects they exert on postsynaptic neurons, but very little is known of the details of their form. In view of the diverse targets of projections of ICC neurons, study of the structure of axon terminals raises several questions. Do the axonal terminals of ICC neurons differ among the target nuclei, either within the MGB or across the range of nuclei receiving its projections? Do single ICC axons project to multiple targets? How might these different patterns of input shape the physiological responses of postsynaptic neurons?

MATERIALS AND METHODS

Deposits of anterograde tracers were placed within physiologically defined regions of the inferior colliculus in se-

Abbreviations

ALD	anterolateral division of the central nucleus of the inferior colliculus	MD	medial division of the central nucleus of the inferior colliculus
Am	amygdala	MGB	medial geniculate body
BIC	brachium of the inferior colliculus	MRF	mesencephalic reticular formation
BICNl	nucleus of the brachium of the inferior colliculus, lateral part	PcT	pericollicular tegmentum
BICNm	nucleus of the brachium of the inferior colliculus, medial part	PG	pontine gray
Cb	cerebellum	PGdl	dorsolateral nucleus of the pontine gray
CF	constant frequency	PHA-L	<i>Phaseolus vulgaris</i> -leucoagglutinin
CF _n	<i>n</i> th harmonic of constant frequency biosonar component	Pt	pretectum
CG	central gray	Pyr	pyramid
CIC	commissure of the inferior colliculus	Q _{10dB}	tuning sharpness expressed as best frequency divided by the bandwidth 10 dB above threshold
CP	cerebral peduncle	Ret	thalamic reticular nucleus
CSC	commissure of the superior colliculus	RP	rostral pole nucleus of the medial geniculate body
D	dorsal nucleus or dorsal division of the medial geniculate body	SC	superior colliculus
DAB	diaminobenzidine	Sg	supragenulate nucleus of the medial geniculate body
DC	dorsal cortex of inferior colliculus	SN	substantia nigra
DNLL	dorsal nucleus of the lateral lemniscus	TMB	tetramethylbenzidine
DPD	dorsoposterior division of the central nucleus of the inferior colliculus	V	ventral division of the medial geniculate body
DS	superficial dorsal nucleus of the medial geniculate body	VI	lateral part of the ventral division of the medial geniculate body
Ex	external nucleus of the inferior colliculus	Vm	medial part of the ventral division of the medial geniculate body
FM	frequency modulated	VNLLd	ventral nucleus of the lateral lemniscus, dorsal part
FM _n	<i>n</i> th harmonic of frequency modulated biosonar component	VNLLv	ventral nucleus of the lateral lemniscus, ventral part
Ha	habenula	WGA-HRP	wheat germ agglutinin conjugated to horseradish peroxidase
HRP	horseradish peroxidase		
Hyp	hypothalamus	Planes of section:	
IC	inferior colliculus	D	dorsal
ICC	central nucleus of the inferior colliculus	L	lateral
INLL	intermediate nucleus of the lateral lemniscus	M	medial
M	medial division of the medial geniculate body	V	ventral

dated, locally anesthetized, greater mustached bats (*Pteronotus parnellii parnellii*). Fourteen bats, captured in Jamaica, West Indies, were used in this study. All procedures on the animals were approved by Institutional Animal Care and Use Committees.

Surgical procedures

The dorsal surface of the inferior colliculus was exposed in bats anesthetized with methoxyflurane (Metofane, Pitman-Moore, Inc., Mundelein, IL) and sodium pentobarbital (10 mg/kg, i.p.; Nembutal, Abbott Laboratories, North Chicago, IL). A midline incision was made in the skin overlying the skull and the muscles were reflected laterally. A sharpened tungsten ground electrode was cemented into the right cerebral cortex, and a small hole was drilled in the skull over the left inferior colliculus (IC). A long-lasting local anesthetic, lidocaine (Elkins-Sinns, Inc., Cherry Hill, NJ), was then applied to the surgical wounds. The bat was placed in a plexiglas restraining apparatus in a heated and humidified experimental chamber. A bite bar oriented the head in a uniform position, which was fixed by cementing a pin to the skull and securing the pin to the restraining apparatus. Data collection began after recovery from the general anesthetic. Light sedation, in which animals were awake but quiescent, was maintained with a cocktail of Nembutal (5 mg/kg) and acepromazine (2 mg/kg, s.c.; Med-Tech, Inc., Buffalo, NY). Animals were also given occasional injections of a 5% dextrose solution to maintain appropriate energy and water balance.

Acoustic stimulation and recording procedures

Tone bursts (30 msec duration, 1 msec rise-fall times, 3–4/sec) were generated by shaping the output of a function generator (Tektronics model FG 502) with an electronic switch (Wilsonics model BSIT). The sine wave frequency was monitored with a frequency counter accurate to ± 5 Hz. The output of the electronic switch was connected, via an impedance matching network, to an attenuator (Hewlett Packard model 350D), and its output was fed into a Polaroid (model T2004) condenser speaker, with a 180 VDC polarization. The speaker, fitted with a funnel ending in a 6 mm (inside diameter) tube, was placed within the pinna but not into the external auditory meatus of the ear contralateral to the recording site.

The evoked activity of multiunit clusters was recorded with micropipettes having tip diameters of 5–10 μm (resistances of 0.5–3 Megohms). Micropipettes were filled with either phosphate buffered saline (0.9 M NaCl, 0.1 M phosphate buffer, pH 7.6) and 30% horseradish peroxidase (HRP; type VI, Sigma Chemical Co., St. Louis, MO), or citrate buffer (0.1 M, pH 5.0) with 50 $\mu\text{Ci}/\mu\text{l}$ [^3H]leucine (New England Nuclear, Boston, MA). Electrodes were advanced by a Narishige hydraulic micropositioner controlled outside the experimental chamber. Extracellular action potentials were filtered (bandpass, 500–3,000 Hz), amplified by conventional means, and sent through a window discriminator (Frederick Haer and Co. model 74-60-3) for audiovisual display. Multiunit responses that were analyzed consisted of stimulus-locked clusters of clearly defined spikes. The threshold of the window discriminator was adjusted to detect spike activity exceeding the baseline noise level.

Using the surface vasculature as a guide, electrodes were placed visually to record neural activity within the ICC. Multiunit responses were usually sampled at 100 μm

intervals. Response properties were evaluated using tone bursts presented to the contralateral ear. The best frequency (the frequency requiring the lowest intensity to elicit stimulus-locked spikes) and threshold at best frequency (defined as the lowest intensity required to elicit one or more spikes to each of five consecutive stimuli) were measured for each cluster. In most cases, the $Q_{10\text{dB}}$ measure of tuning sharpness was obtained at the deposit site, since very sharp tuning distinguishes ICC neurons analyzing some components of the biosonar signal (Pollak and Bodenhamer, 1981; O'Neill, 1985).

At the end of a penetration, response properties were again characterized in the region to receive the iontophoretic deposit, usually at 50 μm intervals. Iontophoretic deposits of HRP were made using a constant current source (Midgard model CS3) with a continuous positive current (1.0–1.5 μAmp) for 20–30 minutes. Iontophoretic deposits of [^3H]leucine were made using pulsed positive current (1.0 μA , 7 seconds on/off cycle) for 10 minutes. The electrode was left in place for 5 minutes after the deposit, and then withdrawn from the brain or moved to another deposit site within the penetration.

Histology

After tracer deposits, the bat received additional lidocaine, its surgical wound was sutured, and it was returned to its holding cage. The animal was perfused 22–30 hours after the first deposit was made, after having been deeply anesthetized with Nembutal (60 mg/kg, i.p.). When nociceptive reflexes were eliminated, the chest cavity was opened and the animal was perfused through the heart with phosphate buffer, a mixed aldehyde fixative (1.25% glutaraldehyde, 1% paraformaldehyde; Mesulam, 1982), followed by a cold (4°C) solution of 10% sucrose in phosphate buffer. After 1 hour, the brain case was opened, and the brain was blocked in a consistent plane (the plane of most electrode penetrations), inclined about 15° from dorsal and caudal to ventral and rostral. This plane is consistent with previous physiological studies of the IC (Wenstrup et al., 1986, 1988a). The brain was refrigerated overnight in a 30% sucrose-phosphate buffer solution.

The brain was sectioned transversely on a freezing microtome at a thickness of 30 μm . All sections between the cochlear nuclei and the auditory cortex were collected into cold 0.1 M phosphate buffer. Every third section was processed by a different protocol. The first series was processed using tetramethylbenzidine (TMB) as chromogen and counterstained with neutral red (Mesulam, 1982). In experiments not involving [^3H]leucine deposits, both the second and third series were processed using a heavy metal intensification of the diaminobenzidine (DAB) reaction (Adams, 1981). Sections from a DAB series were cleared and coverslipped, while others were stained with cresyl violet and then coverslipped.

In four HRP experiments, two or three deposits of [^3H]leucine were made elsewhere in the ipsilateral IC. The third series of sections was prepared for autoradiography as described previously (Cowan et al., 1972). Sections were mounted onto gelatinized slides, defatted, and dried. Under sodium safelight illumination, the slides were dipped in liquid photographic emulsion (NTB2, Eastman Kodak Co., Rochester, NY) at 45°C, dried in a humidified chamber, and then packed with desiccant in light-tight boxes and stored at 4°C for 3–4 weeks. The autoradiographs were developed in D-19 (Kodak) for 3 minutes at 15°C and fixed with rapid

fixer (Kodak; without hardener). The sections were then counterstained for Nissl substance with cresylecht violet and coverslipped.

Other tracers were used in two animals to corroborate results of earlier HRP experiments; the procedures are briefly described here. In one bat, we placed two deposits of wheat germ agglutinin conjugated to HRP (WGA-HRP, Sigma Chemical Co.) and two deposits of *Phaseolus vulgaris* leucoagglutinin (PHA-L, Vector Laboratories, Burlingame, CA). Iontophoresis and histochemistry of WGA-HRP followed the HRP protocol, except that electrodes were filled with 2% WGA-HRP and current (1.0 μ A, electrode positive) was applied for 20 minutes (50% duty cycle). Iontophoresis and immunohistochemistry of PHA-L followed the protocol of Gerfen and Sawchenko (1984) with the following exceptions. A double-barreled electrode, broken to a tip diameter of 10 μ m for each barrel, was used to record physiological responses (0.5 M NaCl) and iontophoretically deposit PHA-L (2.5% in 10 mM phosphate buffered saline). The PHA-L deposits were made first, and the WGA-HRP deposits were made 5 days later. After an additional day, the animal was perfused with a mixed aldehyde fixative (1.25% glutaraldehyde, 1% paraformaldehyde). Anterogradely transported PHA-L was visualized by using the avidin-biotin immunoperoxidase procedure (Vectastain ABC kit, Vector Laboratories) on sections pretreated with a 10% methanol/3% hydrogen peroxide solution to quench WGA-HRP enzymatic activity.

In an additional animal, multiple deposits of biocytin (Sigma Chemical Co.) were placed in each IC. Electrodes with tip diameters of 5–10 μ m were filled with 5% biocytin in phosphate buffered saline (0.9 M NaCl, 0.1 M phosphate buffer, pH 7.6). Biocytin was iontophoresed using +5 μ A continuous current for 10 minutes. The animal was perfused (2% paraformaldehyde, 0.5% glutaraldehyde) 1–2 days after the deposits, and biocytin was visualized using the avidin-biotin peroxidase procedure (Vector Laboratories).

Data analysis

The HRP iontophoresis parameters used here favored the extensive filling of neurons, probably by diffusion (Mesulam, 1982). Thus, DAB-reacted sections contained diffuse, agranular labeling of axons and presumptive axon terminals (Fig. 11), similar to procedures using PHA-L (Gerfen and Sawchenko, 1984) or biocytin (King et al., 1989; Izzo, 1991). In TMB-reacted tissue, the fine granular anterograde labeling, presumably reflecting cellular transport mechanisms, was also seen. However, the diffusely labeled axons in DAB-reacted sections allowed us to relate the location and shape of terminal boutons with cytoarchitectonic subdivisions, and we chose to display these primarily.

To show HRP deposit sites, we illustrate both the central core of dense HRP reaction product and a surrounding zone containing nearly all diffusely labeled perikarya. The latter measure may be the best estimate of the effective uptake zone for anterograde diffusion. Because axons passing through the injection site were probably damaged (Mesulam, 1982), and because they were likely to be filled by HRP in both directions, we examined regions of the IC that may send axons through the injection site for diffusely labeled somata. In each case description, the location of diffusely labeled cells in ICC regions remote from the injection site is noted. We also compared the pattern of transport from

different frequency representations to determine whether damaged axons of passage could explain our results and conclusions. In frequency representations in which damage to axons of passage might be a factor, we also conducted tracer experiments with [3 H]leucine or WGA-HRP. The former is believed to be taken up and transported only by cell bodies (Edwards and Hendrickson, 1981).

As a separate check on the limits of the deposit sites, we analyzed the distribution of retrograde labeling in the nuclei of the lateral lemniscus in DAB-processed sections, examining whether labeling was restricted and whether a tonotopic pattern could be discerned across experiments. However, the uptake zone for retrograde neuronal mechanisms is probably not the same as the zone for anterograde filling; the latter seemed more restricted. Thus, in some experiments, TMB-processed retrograde labeling was widespread throughout nuclei of the lateral lemniscus, while TMB- or DAB-processed anterograde material was more restricted. We chose DAB-processed material to provide an indication of the center of the deposit site.

For diffusely labeled axons, there was little difference in sensitivity using DAB and TMB methods, but the DAB material revealed the form of presumptive axon terminals (Fig. 11). Although we could not establish whether these structures are in fact synaptic terminals, studies of auditory nerve terminals in the cochlear nucleus (Rouiller et al., 1986) and medial lemniscal terminals in the ventrobasal complex (Rainey and Jones, 1983) suggest that HRP-labeled boutons observed in light microscopy correspond to synaptic terminals seen in the electron microscope. In representative DAB-processed sections throughout the ipsilateral MGB, terminal labeling was plotted ($\times 586$, N.A. 0.65, planapochromat) with the aid of a drawing tube. At this magnification, terminals were readily detected and distinguished from perivascular reaction product or other artifacts. Nevertheless, each section was checked at higher power ($\times 937$) to ensure that all clearly identifiable terminals were included. Each plot was compared with its adjacent TMB-processed section to determine the correspondence between the procedures.

Terminal and preterminal labeled axon segments were drawn from DAB-processed, Nissl-counterstained sections at high power ($\times 1,875$, N.A. 1.25, planachromat). Every terminal was drawn, but some preterminal branches were omitted for clarity.

Deposit sites of [3 H]leucine were drawn from sections under darkfield illumination. Both the region containing the highest density of silver grains and a larger area where silver grains aggregated over cell bodies are illustrated. Anterograde transport in MGB was analyzed quantitatively. Silver grains within 1,244 μ m²-squares were counted under darkfield illumination at medium power ($\times 312$, N.A. 0.46, planachromat). Background labeling was measured in the contralateral MGB, because HRP experiments showed no projection from the contralateral ICC. The mean background was estimated from 80–120 squares distributed throughout the MGB; the mean was always less than 5 grains/1,244 μ m². Samples in the ipsilateral MGB were considered to be above signal "threshold" when the grain count exceeded the mean in the contralateral MGB by 2.33 times the standard deviation. Counts were excluded over blood vessels and other areas where local irregularities in the emulsion increased the background level. Grain counts in the ipsilateral MGB were then divided into four categories: background, 1–1.9 times threshold, 2–3.9 times thresh-

old, and ≥ 4 times threshold. No attempt was made to distinguish in the counts between terminal and axonal labeling. This was evaluated by comparison with the results from HRP labeling experiments.

RESULTS

Anterograde tracers were placed within physiologically defined regions of the tonotopically organized ICC, centered within frequency bands analyzing major and distinct components of the bat's sonar signal. The correspondence in the ICC among the tonotopic organization, biosonar representation, and tracer deposit sites appears in Figure 1. Briefly, the bat's audible range has a single tonotopic representation that fills three ICC divisions (Fig. 1A): the anterolateral (ALD: 10–59 kHz), the dorsoposterior (DPD: 60–63 kHz), and the medial (MD: 64–120 kHz) (Zook et al., 1985; O'Neill et al., 1989; this study). The elements of the biosonar signal are represented within the ICC tonotopy (Fig. 1B and inset) and include the fundamental of the constant frequency (CF_1 , ~ 30 kHz) and frequency modulated sweep (FM_1 , 30–24 kHz), and several higher harmonics: CF_2 (~ 60 kHz), CF_3 (~ 90 kHz), CF_4 (~ 120 kHz), FM_2 (60–48 kHz), FM_3 (90–72 kHz), and FM_4 (120–96 kHz) (Novick, 1963). Thus, the anterolateral division includes frequency band representations associated with FM_1 , CF_1 , and FM_2 components, the large dorsoposterior division exclusively represents frequencies in the very narrow band associated with the specialized CF_2 ("60 kHz") component, and the medial division includes frequency band representations associated with FM_3 , CF_3 , and FM_4 components (Fig. 1B). (Although biosonar components are used in this paper as a shorthand designation for their affiliated frequency bands and ICC representations, we recognize that these representations may also analyze nonsonar acoustic signals, e.g., social communication calls.)

Deposit sites were centered at frequencies near 25, 30, 55, 61, 80, and 93 kHz (Fig. 1B, Table 1), representing components in the fundamental, second harmonic, and third harmonic of the sonar pulse. Multiple deposits were placed within a given frequency representation to label maximally its efferent projections while limiting tracer uptake in nearby frequency representations. Individual HRP, biocytin, or PHA-L deposits were always resolvable in DAB-processed material; the zone of dense reaction product ranged from < 100 to $250 \mu\text{m}$ in diameter (Fig. 1C). However, a larger area contained diffusely labeled somata that may approximate the effective uptake zone more closely. Deposits of [^3H]leucine were too closely spaced to be resolved. The total size of the leucine deposit zones ranged from about 600 to $1,000 \mu\text{m}$ in diameter (Fig. 1D).

In each experiment, anterograde labeling occurred in several brain nuclei. The most consistent targets were the medial geniculate body and the cell masses of the ventral pons. Input to the pretectum, the external nucleus of the IC, the pericollular tegmentum, the nucleus of the brachium of the IC, and the contralateral IC was variable, depending on the location and frequency tuning of deposit sites. Other targets had generally weaker labeling, including the ipsilateral superior colliculus and an assortment of brain stem auditory nuclei.

Labeling in the medial geniculate body

Tectothalamic input shared certain features across experiments. First, the projection to the MGB was exclusively

ipsilateral. Second, each of the major divisions of MGB was labeled. Third, the projections to the ventral division from ICC frequency representations formed a tonotopic pattern, whereby lower frequencies projected laterally and higher frequencies projected successively more medially and rostrally.

Projections from 25–30 kHz. ICC representations of the CF_1 (~ 30 kHz) and FM_1 (25–30 kHz) sonar components are small and in close proximity. Tracer deposits in one of these are likely to spread to the other as well; we therefore consider them jointly. This description of low frequency projections relies on autoradiographic cases (Fig. 2), because HRP deposits damaged tectothalamic fibers from other ICC divisions (see below). HRP data (Fig. 3) reveal the pattern of terminal labeling at MGB loci where silver grains were concentrated in autoradiographic experiments.

Deposits of [^3H]leucine were placed near 25 kHz in two bats, and at 30–33 kHz in two others. Transport was qualitatively similar, probably because the deposit sites filled both representations. In the case illustrated (Fig. 2), three [^3H]leucine deposits were made at 25.6 kHz (Figs. 1D, 2G). The total deposit zone was large, encompassing much of the rostrocaudal extent of the 25 kHz representation, but also including frequencies from about 17 to 40 kHz within the anterolateral division of ICC.

Dense accumulations of silver grains were observed in all divisions of MGB (Fig. 2). Invariably, the heaviest labeling occurred within a group of MGB subdivisions located nearer to the perimeter of MGB. These include the suprageniculate nucleus, the medial division, the lateral subdivision of the ventral nucleus (Vl), the dorsal nucleus, and the ventromedial extreme of the rostral pole nucleus. Nuclei within the central part of MGB, including the medial subdivision of the ventral nucleus (Vm) and most of the rostral pole nucleus, were labeled only very lightly, and some of this label was clearly preterminal (Fig. 2D, unfilled arrow). However, a few small patches are probably terminal labeling (Fig. 2D–F, filled arrows), so a minor input to Vm and the rostral pole cannot be excluded. Nonetheless, the results of all autoradiographic experiments show that several subdivisions along the margin of MGB receive the bulk of input from low frequency representations in ICC; high frequency ICC inputs formed a conspicuously different pattern (see below).

The brachium of the IC and the pretectum were also labeled. Much of the brachial labeling was preterminal (Fig. 2A, unfilled arrow), while that in the pretectum was probably terminal labeling (Fig. 2C,D, filled arrows) since it lies outside the path of brachial axons.

Results from HRP deposits near 30 kHz in two animals were similar to each other. Figure 3 presents a case in which three HRP deposits were placed in the caudal half of the 30–33 kHz representation (Fig. 3G). Retrograde labeling in the nuclei of the lateral lemniscus (Fig. 3H) and contralateral IC (not shown) verified that deposits were centered in low frequency representations of ICC. However, there were several diffusely labeled cells in the ipsilateral medial division of ICC, many in the region representing FM_3 and CF_3 biosonar components. This indicates that tectothalamic fibers originating in the medial division were damaged as they passed through the 30–33 kHz region. Thus, several labeled axons in MGB probably originated from cells tuned to frequencies above 64 kHz, some within FM_3 and CF_3 frequency bands.

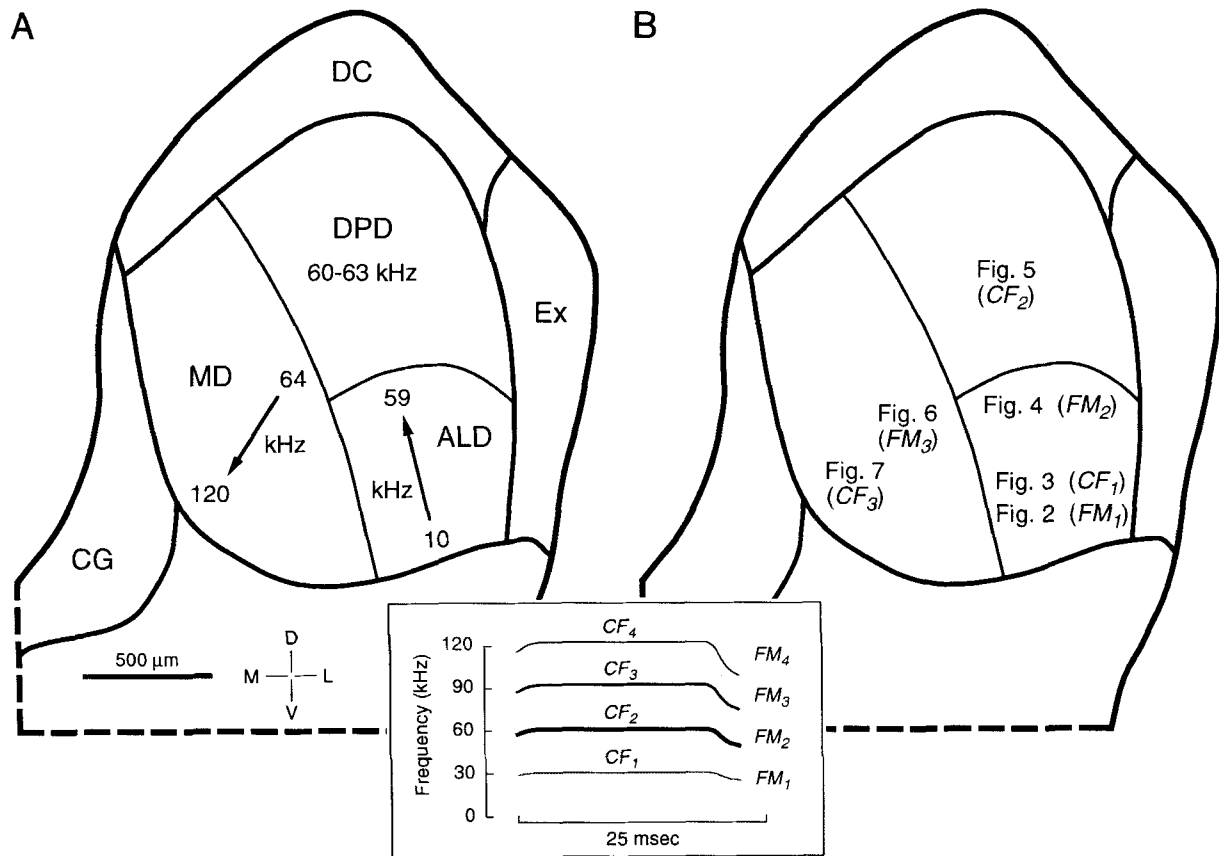


Fig. 1. Organization and tracer deposits in the mustached bat's inferior colliculus. **A:** Tonotopic and architectonic organization. **B:** Schematic localization of ICC tracer deposits illustrated in Figures 2-7, and the biosonar components (in parentheses) represented by frequency bands in which deposits were placed. Only projections of frequencies analyzing the first three harmonic elements were studied. **C:** Photomicrograph of inferior colliculus showing two iontophoretic

deposits of HRP placed at sites sharply tuned near 62 kHz. Heavy metal-intensified DAB chromogen. See also Figure 5G. **D:** Darkfield photomicrograph of [³H]leucine deposit zone resulting from three iontophoretic deposits at sites tuned near 25 kHz. See also Figure 2G. Protocol for C, D. planachromat, N.A. 0.08, ×100. **Inset:** Sonogram of mustached bat biosonar pulse with signal components labeled.

TABLE 1. Summary of Frequency Tuning and Tracers at ICC Deposit Sites

Experiment no.	BF at deposit sites (kHz)	Tracer	No. of deposits	Figure
1002-1	25.4–25.8	[³ H]leucine	2	—
1010-1	25.5–25.6	[³ H]leucine	3	1D, 2
966	30.3–33.4	HRP	3	3, 11D, 12B
980	33.3–33.4	HRP	3	—
984-1	30.2–30.5	[³ H]leucine	2	—
987-1	30.0–33.4	[³ H]leucine	3	8A,B
1002-2	53.1–54.5	HRP	4	—
N6-1	53.5–56.0	WGA-HRP	2	4
N54-1	52.0–54.5	Biocytin	5	—
954	60–64 ¹	HRP	2	—
971	60.0–60.2	HRP	3	—
984	61.6–62.3	HRP	6	1C, 5, 8C,D, 9A,B, 10, 11A–C, 12A,E,F, 13A,C,D
1010-2	77.6–81.6	HRP	4	12D, 13B
N6-2	82.5–83.5	PHA-L	2	—
N54-2	82.6–83.7	Biocytin	4	6, 8E,F
965	92.4–92.7	HRP	3	7, 9C,D, 12C
969	92.8	HRP	1	—
987	93.0–94.4	HRP	4	8A,B

¹Estimate only; no physiological recording; deposits confined to DPD.

Terminal labeling was observed in all divisions of MGB (Fig. 3). Targets included VI, the suprageniculate nucleus, the medial division, the dorsal and superficial dorsal nuclei, and the ventromedial extreme of the rostral pole. The pretectum was also labeled. These inputs recapitulated the pattern seen in the autoradiographic experiments. The major difference from autoradiographic experiments was the occurrence of more extensive clusters of labeling in Vm and the rostral pole nucleus (Fig. 3A–E). This labeling was consistent with the effects of damage to high frequency FM₃ and CF₃ tectothalamic axons (see Figs. 6, 7).

In both HRP and autoradiographic experiments, the distribution of 25–30 kHz input in the ventral and suprageniculate nuclei formed part of the tonotopic arrangements. In VI, small patches of terminal labeling lay between the lateral and medial borders, occurring along much of its caudorostral extent (Figs. 3A–E, 12B). Viewed in serial sections, this terminal field took the form of a more or less dorsoventrally oriented, patchy sheet of terminals that was congruent with the laminar arrangement of principal cell dendrites in Golgi material (Winer and Wenstrup, 1994b). Autoradiographic experiments (Fig. 2A–E) support the dorsoventral frequency representation, although the labeling was less patchy and more broadly distributed in VI from these larger deposit sites. In the suprageniculate nucleus, only the lateral and dorsal parts were labeled heavily (Figs. 2A,B, 3A,B).

Projections from 50 kHz. Frequencies in the 48–60 kHz range, representing the FM₂ sonar component, occupy an expanded representation in the caudal and dorsal part of the anterolateral division of the ICC (O'Neill et al., 1989). Three experiments examined tectothalamic projections of this region. In one (Fig. 4), two large deposits of WGA-HRP were placed at sites tuned near 55 kHz, in the caudal and middle parts of this representation (Fig. 4G). Retrograde labeling in the nuclei of the lateral lemniscus was highly restricted (Fig. 4H), and it appeared to abut labeling in 60 kHz cases (see Fig. 5H). In one HRP case and one biocytin case, deposit sites and thalamic labeling were more restricted, but they corroborated the major projections illustrated here.

In MGB, targets of 50 kHz input were widespread and included all divisions (Fig. 4). Within the caudal half, however, intense labeling occurred only in the suprageniculate nucleus (Fig. 4A,B). Ventral division labeling was light

to moderate in VI, located nearer its medial face and extending throughout its rostrocaudal extent. A dorsoventrally oriented strip of label was sometimes present (Fig. 4B,D,E), a pattern recalling the laminar arrangement of principal cell tufted dendrites in Golgi preparations (Winer and Wenstrup, 1994b) and perhaps contributing to tonotopically organized input from ICC. Light label was also present along the medial border of Vm (Fig. 4B). The 50 kHz tectothalamic input to the ventral division was significantly lighter than that originating from most other frequency bands.

Most labeling lay in the rostral half of the MGB, covering much of the rostral pole nucleus and the dorsal division. Two distinct patches were seen, one placed ventrally in the rostral pole nucleus and another spanning it and the dorsal division (Fig. 4C–F). These bore no clear relationship to a tonotopic organization. There was also light labeling in the medial division and the pretectum (Fig. 4B–D).

Projections from 60 kHz. Frequencies between 60 and 64 kHz represent the CF₂ sonar component and have a massive ICC representation as the distinct dorsoposterior division (Zook et al., 1985; O'Neill et al., 1989). Results from three HRP experiments were available. In two, the deposits were large or numerous, and the results were similar. The third case involved deposits limited to the dorsal part, and anterograde label was distributed within a subset of the MGB regions labeled in the two other experiments.

Six iontophoretic deposits of HRP were made in one experiment (Fig. 5G). Responses at deposit sites were tuned between 61.7 and 62.3 kHz and had characteristically high Q_{10dB} values of 62–123. Only the most rostral part of the 60 kHz region lay beyond the deposit zone. A few diffusely labeled cells lay in the medial division of ICC, but many fewer than in the 30 kHz HRP case (Fig. 3). Thus, some MGB label may reflect damage to ICC neurons tuned above 64 kHz, possibly within FM₃ and CF₃ frequency bands.

Most labeled cells in the nuclei of the lateral lemniscus were clustered in regions known to represent 60 kHz (Fig. 5H) (Ross et al., 1988). In the dorsal nucleus, they formed a band centered between the dorsal and ventral borders. In the intermediate nucleus, they lay in the dorsolateral part, and in the ventral nucleus they formed bands that were oriented horizontally, across the path of lemniscal fibers.

Fig. 2. (See overleaf.) Results of a 25 kHz (FM₁) autoradiographic experiment. **A–F:** Distribution of silver grains in MGB from three deposits of [³H]leucine. The heaviest labeling occurred in nuclei along the perimeter of MGB, including the ventral division (VI), suprageniculate nucleus (Sg), lateral part of the dorsal nucleus (D), medial division (M), and ventromedial part of the rostral pole (RP). Labeling generally avoided the medial part of the ventral division (Vm) and the rostral pole nucleus (RP). Size of dots, density of silver grains within 35 μm × 35 μm squares, from > 1× threshold (smallest dots), to > 2× threshold (medium dots), to > 4× threshold (largest dots). Filled arrows indicate selected regions of presumptive terminal labeling within MGB, while unfilled arrows indicate like areas of presumptive preterminal labeling. Numbers at lower left in MGB sections indicate the distance from the caudal tip of the MGB as a fraction of the total caudal-to-rostral dimension. **G:** [³H]leucine deposit zones and frequency tuning in penetrations through the inferior colliculus. The deposit zone was mostly contained within the ICC. Electrode tracks were not contained within the plane of section. Blackened region, core of the deposit zone; shaded region, area where silver grains accumulated densely over cell bodies. Numbers, best frequencies at recording sites; white-on-black numbers, best frequency at deposit site.

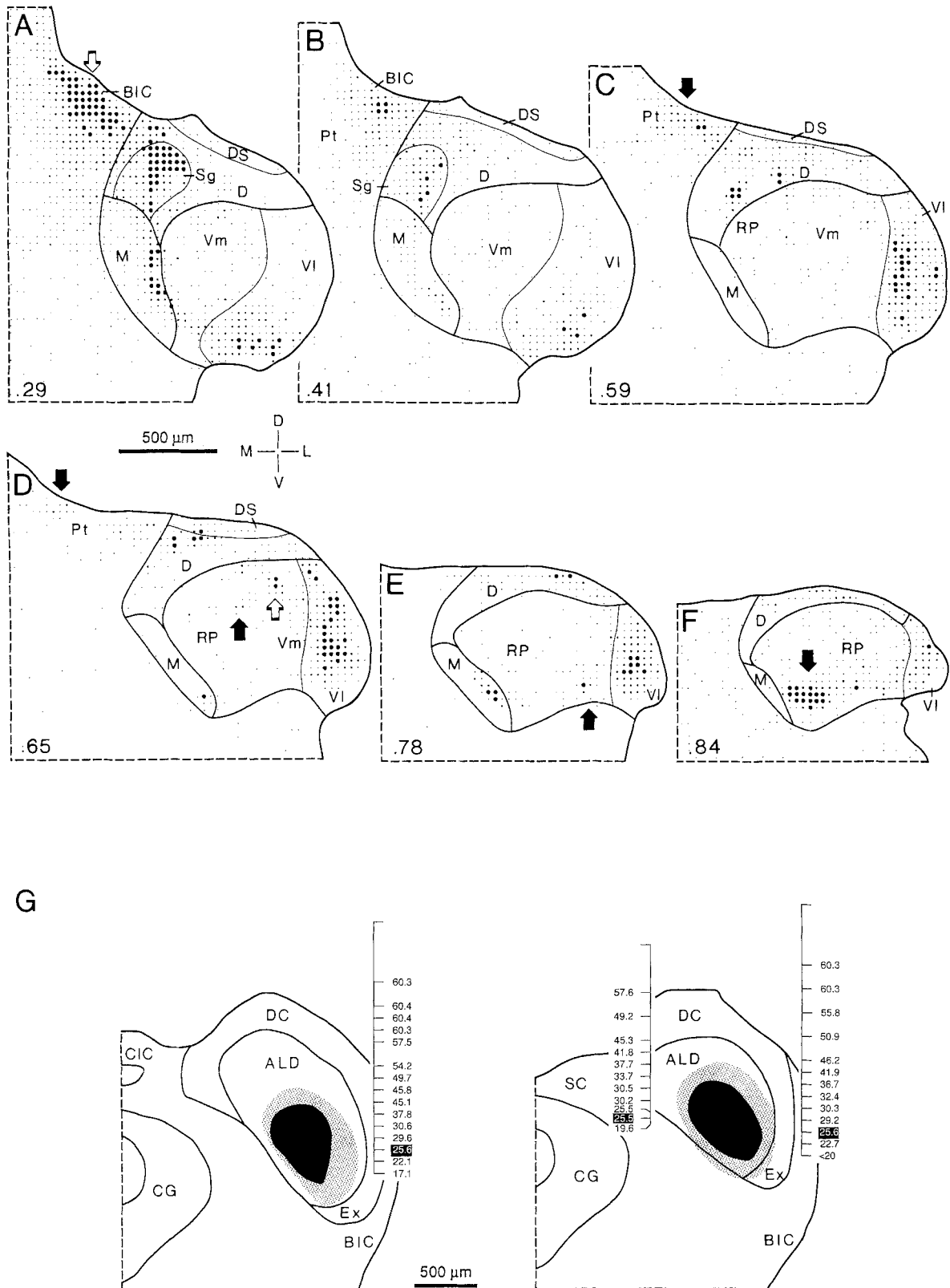


Figure 2 (See legend on previous page.)

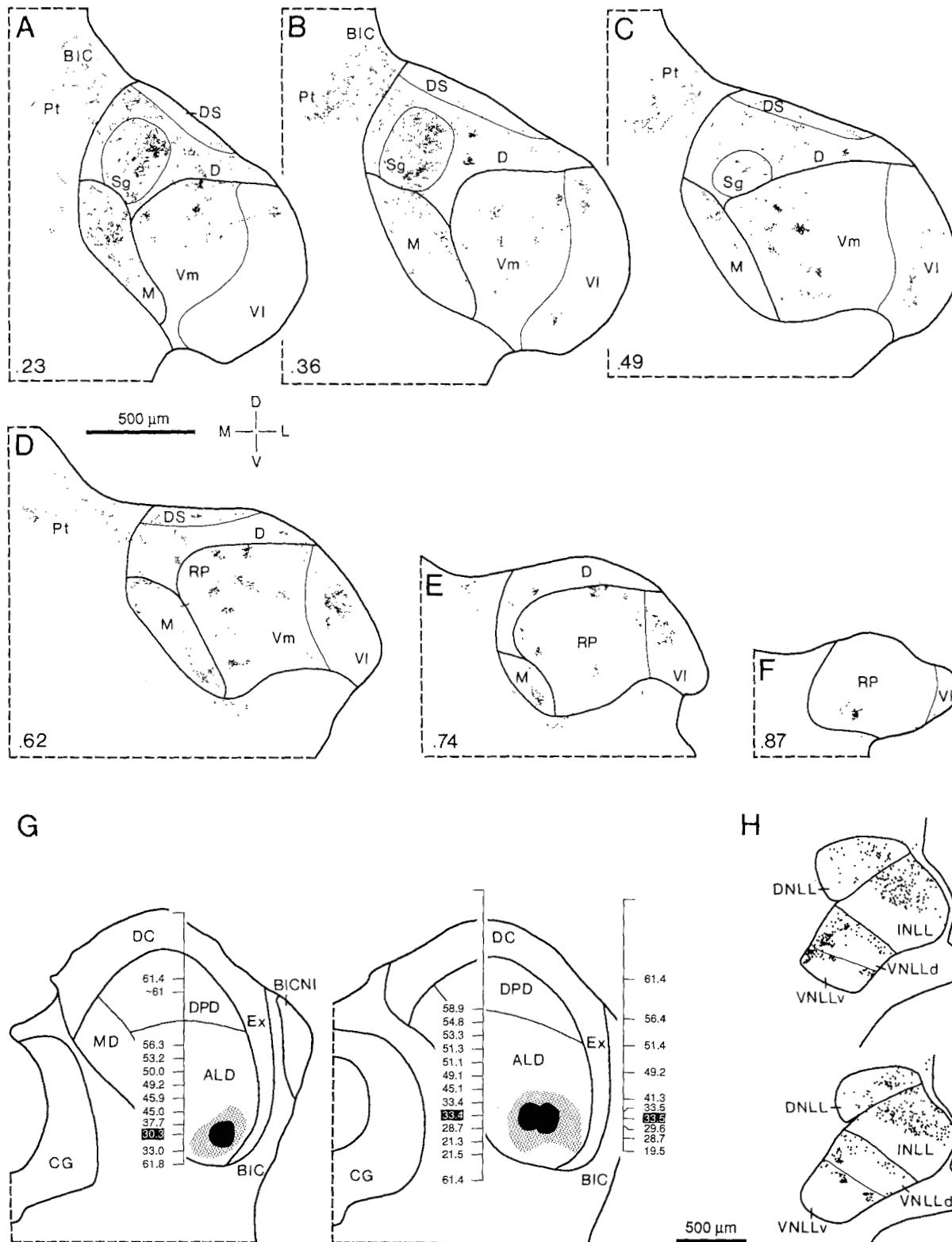


Fig. 3. Results of a 30 kHz (CF₁) HRP experiment. **A-F**: Distribution of labeled boutons (dots) in MGB from three HRP deposits. Labeled areas included those marked by [³H]leucine deposits (Fig. 2), but also included the medial part of the ventral division (Vm) and the rostral pole nucleus (RP). This labeling probably resulted from damage to high frequency axons. **G**: HRP deposit sites and frequency tuning in the inferior colliculus. Same protocol in Figures 3, 5-7. Blackened region shows the core of the deposit zone; shaded region, area within which

most diffusely labeled cells were found. Several diffusely labeled cells were also found more caudally in the medial division of the inferior colliculus, suggesting that some labeling in MGB resulted from damage to high frequency axons passing through the 30 kHz deposit site. Electrode tracks were not contained within the plane of section. **H**: Retrograde label in nuclei of the lateral lemniscus. All sections processed using heavy metal-DAB as chromogen.

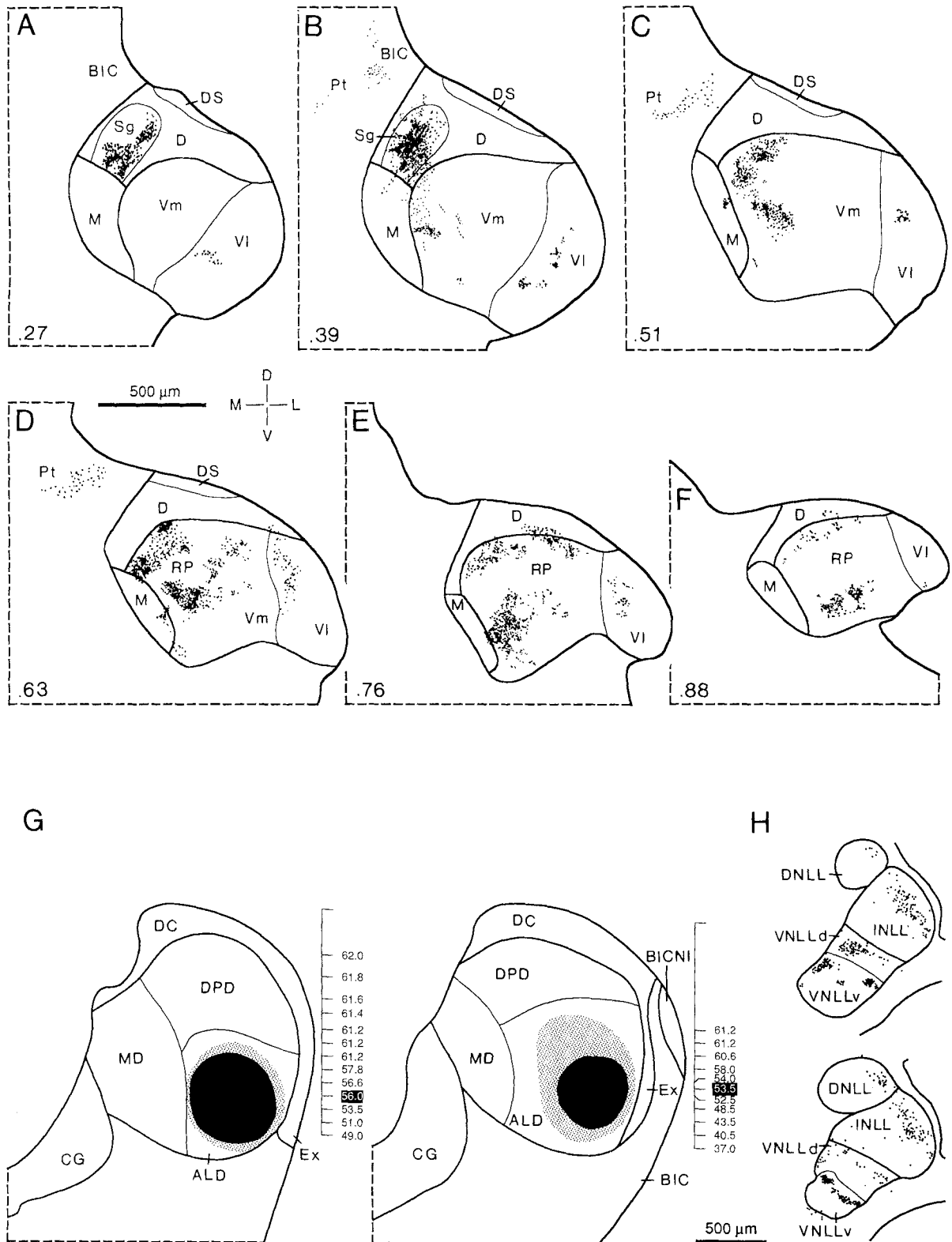


Fig. 4. Results of a 50 kHz (FM_2) WGA-HRP experiment. **A-F:** Distribution of anterograde label (dots) in MGB from two ICC deposits. Most labeling lay in the suprageniculate nucleus (Sg) and the rostral pole nucleus (RP). Weaker input terminated within the lateral part of the ventral division (VI). Section F differs in size and subdivisions from other sections at the same caudal-to-rostral level (Figs. 3F, 6F), possibly due to differences in sectioning. Its appearance suggests a position

slightly caudal to Figures 3F and 6F (see Fig. 2F). **G:** WGA-HRP deposit sites and frequency tuning in the inferior colliculus. Blackened region shows the core of the deposit zone; the shaded region is more lightly labeled, but may lie within the transport zone of the deposit. Electrode tracks were not contained within the plane of section. **H:** Retrograde label in nuclei of the lateral lemniscus. All sections processed using TMB as chromogen.

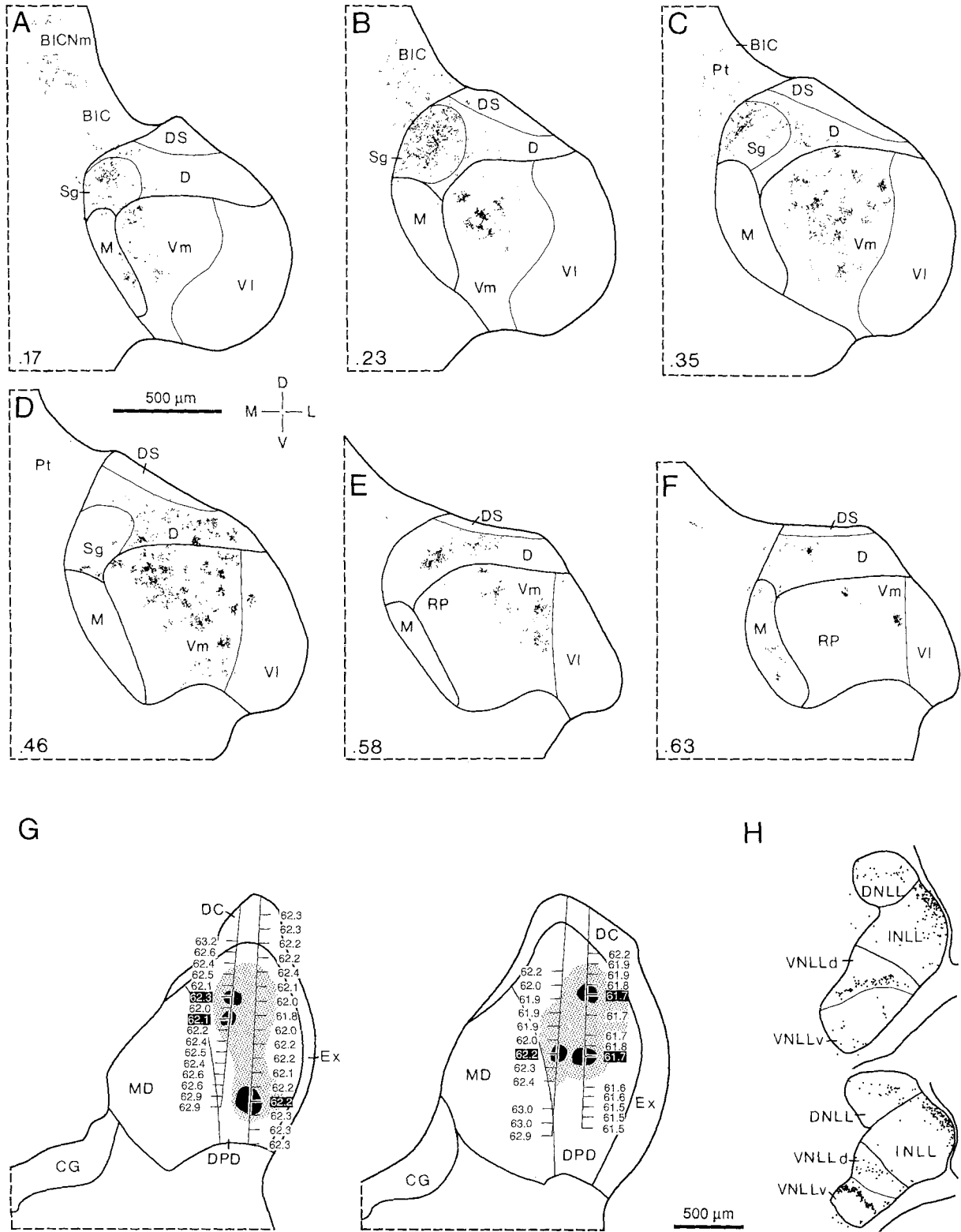


Fig. 5. Results of a 60 kHz (CF₂) HRP experiment. **A-F:** Distribution of labeled boutons (dots) in MGB from six ICC deposits. Heavy input was found in the medial part of the ventral division (Vm), the dorsal nucleus (D), and the supragenulate nucleus (Sg). **G:** HRP deposit sites and frequency tuning in the inferior colliculus. See Figure

3 for protocol. A few diffusely labeled cells were found in the medial division of the inferior colliculus (MD), though many fewer than in the 30 kHz experiment in Figure 3. **H:** Retrograde labeling in nuclei of the lateral lemniscus. All sections processed using heavy metal-DAB as chromogen.

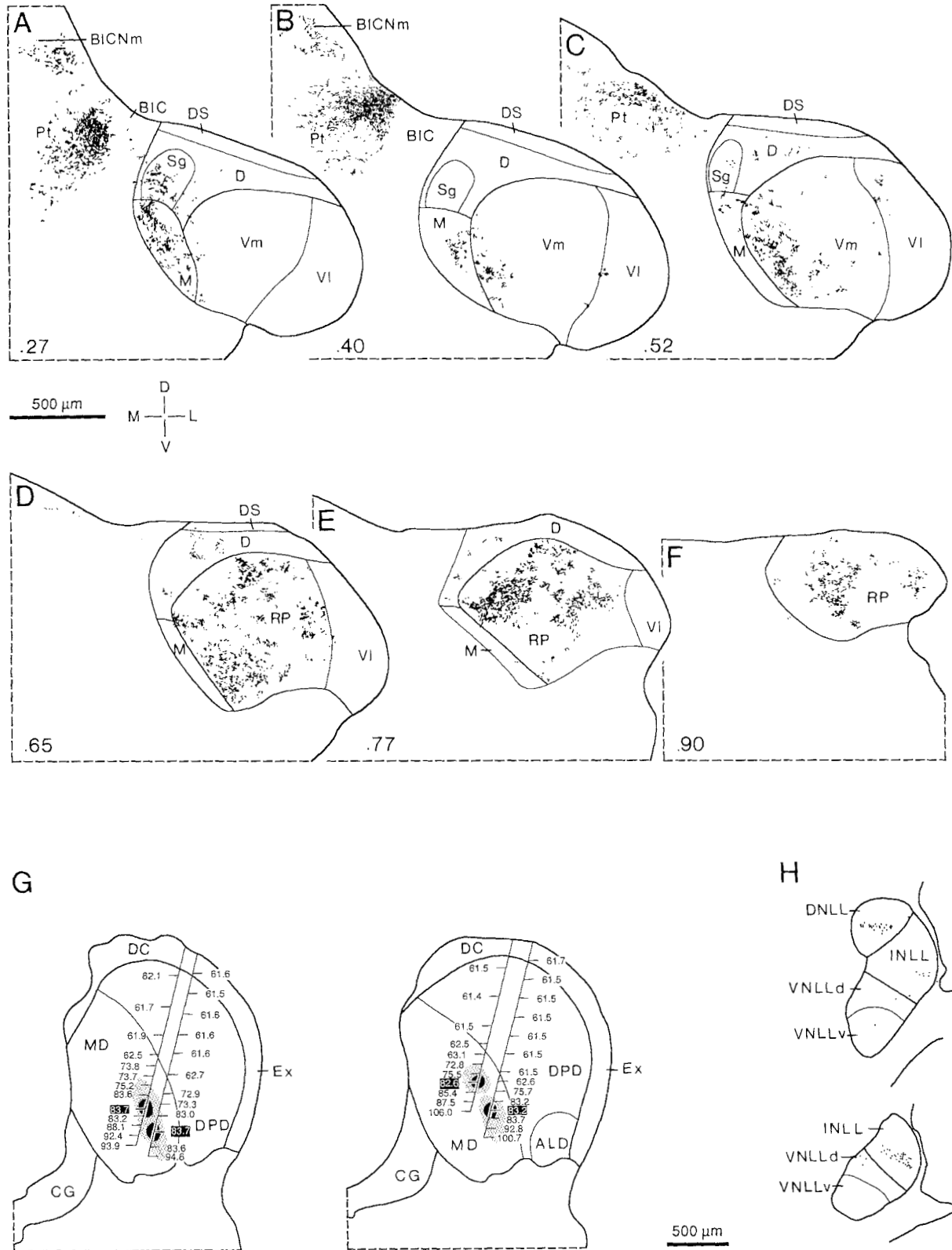


Fig. 6. Results of an 80 kHz (FM₃) biocytin experiment. **A-F:** Distribution of labeled boutons (dots) in MGB from four ICC deposits. Note the intense labeling in the pretectum, a consistent feature of 80 kHz experiments. In MGB, most labeling lay in the rostral pole nucleus (RP), although the medial part of the ventral division (Vm), the

suprageniculate nucleus (Sg), and medial division (M) were at least moderately labeled. **G:** Biocytin deposit sites and frequency tuning in the inferior colliculus. See Figure 3 for protocol. **H:** Retrograde labeling in nuclei of the lateral lemniscus.

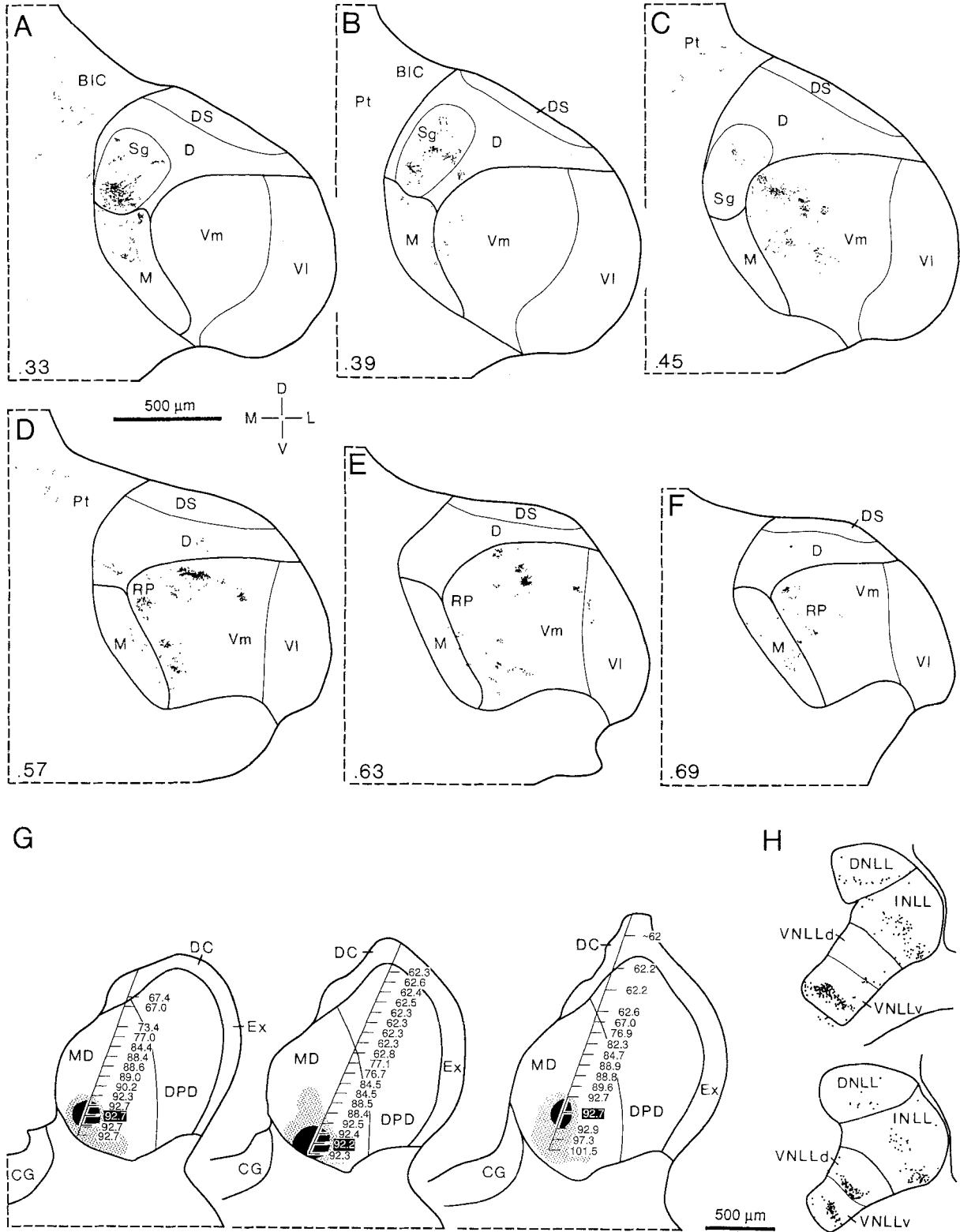


Fig. 7. Results of a 90 kHz (CF₃) HRP experiment. **A-F**: Distribution of labeled boutons (dots) in MGB from three ICC deposits. Most labeling occurred in the medial part of the ventral division (Vm), the supragenulate nucleus (Sg), and the rostral pole nucleus (RP). **G**:

HRP deposit sites and frequency tuning in the inferior colliculus. See Figure 3 for protocol. **H**: Retrograde labeling in nuclei of the lateral lemniscus. All sections processed using heavy metal-DAB as chromogen.

However, in the dorsal part of the ventral nucleus, the bands turned ventromedially, oriented nearly in parallel with the ascending fibers. This orientation was common here (see also Figs. 3H, 4H) and in another study (Frisina et al., 1989), suggesting a complexity in the frequency organization of the ventral nucleus of the lateral lemniscus.

The thalamic targets of 60 kHz ICC input were widespread (Fig. 5A–F). In the ventral division, nearly all terminals lay in Vm, medial to the 50 kHz foci in VI (Fig. 4B,C). The projection extended throughout the caudorostral extent of Vm. Caudally, labeling bordered the medial division (Fig. 5A,B). More rostrally, the labeled region expanded laterally and ventrally (Fig. 5C,D), and there was no labeling at the medial division border. Medially, this region was bounded by higher frequency representations (see below).

Sparse labeling remained rostrally in Vm and the rostral pole nucleus (Fig. 5E,F). Comparison with the FM₃ and CF₃ experiments described below (Figs. 6, 7) suggests that only this part of the labeling in the present experiment could result from damage to neurons in the medial division of ICC. Moreover, since physiological studies have recorded 60 kHz responses in this part of the MGB (Olsen, 1986), we believe much of this labeling represents 60 kHz ICC input.

Several dorsal division nuclei were labeled, particularly the supragenulate nucleus (Fig. 5A–C); more input was found medially than in the 25–30 kHz deposits. This input was far lighter rostrally. The dorsal nucleus had several patches of moderate-to-heavy label concentrated midway through the MGB (Fig. 5D,E), while the superficial dorsal nucleus was virtually unlabeled; in another 60 kHz case, dorsal division labeling extended into the rostral third of MGB. The medial division received only a few patches near its caudal (Fig. 5A) and rostral (Fig. 5F) poles.

Projections from 80 kHz. Frequencies corresponding to the FM₃ sonar component (72–90 kHz) were well represented within the medial division of ICC. The sharpness of tuning was much less than in either the 60 kHz (CF₂) or 90 kHz (CF₃) representations, providing an independent criterion for distinguishing this region from the adjacent 90 kHz representation. Three experiments examined the tectothalamic projections of these frequencies, one each using HRP, biocytin, and PHA-L. Their results agreed well except for some artifactual label in the HRP case.

In the biocytin case, four deposits were placed at sites tuned at 82–84 kHz (Fig. 6G). The deposit sites were highly restricted within the medial division of ICC. Only a few diffusely labeled cells were beyond the deposit sites, and these were in the medial division. Labeling in the nuclei of the lateral lemniscus was restricted to bands in the dorsal and intermediate nuclei, with little in the ventral nucleus (Fig. 6H).

These deposits revealed widespread yet consistent patterns of connections within MGB (Fig. 6A–F). Most labeling occurred in the rostral half, where several intense foci filled much of the rostral pole. Along a caudal-to-rostral sequence, this label formed a curved band near the dorsal part of the rostral pole nucleus (Fig. 6D,E), turning ventrally in the lateral part, near the VI border (Fig. 6E). Dense networks of labeled preterminal axons joined the foci of terminal labeling, and may reflect the extensive axonal branching evident here (Fig. 12D; see also Frisina et al., 1989). In the caudal MGB, labeling occurred in Vm along the border with the medial division (Fig. 6B,C); this input was more medial and more rostral than 60 kHz label. The

supragenulate nucleus and adjacent medial division were moderately labeled, though only in their caudal part (Fig. 6A,B).

A striking result was the dense input to the pretectum (Fig. 6A–C). Although other frequency bands projected to this region, including 25–33 kHz and 50 kHz bands (Figs. 2–4), the density of 80 kHz input to the pretectum was the highest to any ICC target in this experimental series (Figs. 6, 13B).

The 80 kHz, FM₃ projection shared many features with the 50 kHz, FM₂ projection. Each sent to the ventral division in the caudal MGB a consistent input that formed part of a tonotopic pattern, but their contributions were small. In contrast, the rostral half of MGB, particularly the rostral pole nucleus, was dominated by input from these two frequency bands representing FM components of the sonar signal. Moreover, Figures 4 and 6 suggest that their target zones interdigitate or overlap, and that, together, these inputs fill much of the central part of the rostral MGB. Finally, each projected at least moderately to the pretectum.

Projections from 90 kHz. In ICC, the expanded representation of frequencies of the third harmonic, constant frequency sonar component (CF₃, near 93 kHz) was readily distinguished from neighboring frequency representations. On entering this region from lower frequency representations, a jump in best frequency of > 2 kHz was common, after which the best frequency changed very little (< 1 kHz). Exiting the region, electrodes recorded another sharp increase in the best frequency (Fig. 7G). Units near 93 kHz were also more sharply tuned, with Q_{10dB} values ranging from 40 to 132, whereas the 80 kHz representations had Q_{10dB} factors of 10–31.

HRP deposits were placed within the 92–94 kHz representation in three animals. In the two cases analyzed for MGB labeling, the results differed only in degree, probably from differences in the locus of deposit sites. In one case (Fig. 7), three deposits were placed in an ICC region tuned near 93 kHz. Most diffusely labeled cells were confined to the 93 kHz representation, although some lay in higher frequency representations. No diffusely labeled cells were found in the dorsoposterior or anterolateral divisions of ICC, and only a very few were found in regions of the medial division representing frequencies below 90 kHz. In each of the nuclei of the lateral lemniscus, restricted groups of retrogradely labeled cells (Fig. 7H) lay ventrally, further suggesting that deposit sites were located in high frequency representations within ICC.

The 93 kHz ICC representation projected to all three MGB divisions (Fig. 7A–F), as did all frequency bands. Ventral division input formed scattered foci in Vm along the medial division border (Figs. 7C,D, 12C), terminating more rostrally than 80 kHz input; the labeling never extended as far caudally as that from all lower frequency deposits. A second, more rostral focus (Fig. 7D,E) lay dorsally and extended into the rostral pole. The multiple deposit sites precluded a definitive answer to the question of whether the foci are in fact discrete. This dorsal label may adjoin patches of 60 kHz and 80 kHz terminals (see Figs. 5E, 6D). In both 93 kHz cases, patchy label extended further into the rostral pole but was much weaker than in the 80 kHz experiments.

In the dorsal division, input to the supragenulate nucleus was restricted to the ventral part (Fig. 7A,B), in a position different from that seen after 30 or 60 kHz deposits

(see Figs. 2A,B, 3A,B, 5A–C). Very little dorsal nucleus labeling was found. Medial division input was mainly in the caudal part, with little transport rostrally. A few labeled terminals were also seen in the pretectum (Fig. 7C,D) at much lower density than in 80 kHz experiments.

Extrageniculate projections

Several areas outside the auditory thalamus also received input from ICC. Of these, the pretectum had particularly heavy input. Deposits at 80 kHz produced very intense labeling dorsomedial to the MGB (Figs. 6, 13B). Labeling in 50 kHz experiments was consistent, if weaker (Fig. 4); however, another study showed strong 50 kHz input to this region (Frisina et al., 1989). Input from 25–33 kHz was weaker in both autoradiographic and HRP cases (Figs. 2, 3). Deposits at 60 and 90 kHz labeled very few terminals in the pretectum (Figs. 5, 7). These results suggest that this region may receive its major ICC input from frequency bands analyzing FM components of the bat's sonar echoes.

By far the most consistent extrageniculate labeling was in the ipsilateral nuclei of the pontine gray (Fig. 8). Every experiment labeled at least two patches. One was in the dorsolateral pontine nucleus, recognizable by its large, relatively densely packed cells (Fig. 13D), and another lay in the lateral pontine area, with further patches either in the lateral or ventral pontine areas. Labeling was highly restricted and often very intense (Fig. 8C–F). Projections from different frequency bands terminated in different regions, although overlapping input cannot be ruled out. Thus, low frequency label in the dorsolateral nucleus lay ventrally, an observation obscured by extensive preterminal labeling in Figure 8A and B. Input from 50 kHz (not shown) and 60 kHz (Fig. 8C,D) ICC regions ended more laterally and dorsally, while 80 kHz (Fig. 8E,F) and 90 kHz (Fig. 8A,B) projections terminated more medially. In the lateral pontine area, targets for 30 kHz, 60 kHz, and 80 and 90 kHz input were distinct.

In the midbrain, several structures associated with the IC had moderate to intense labeling, some specific to particular frequency bands. The external nucleus of the inferior colliculus was labeled strongly by 60 kHz deposits (Fig. 9A), weakly by 50 kHz deposits (not shown), but not at all by other frequency bands, e.g., 93 kHz (Fig. 9C). Another target, corresponding to the pericolicular tegmentum described in the cat (Morest and Oliver, 1984), was located ventral to the rostral ICC and contained scattered arrangements of cells of all sizes. Most deposits labeled this region, except for 25 and 30 kHz representations that were located so close to the pericolicular tegmentum that anterograde labeling may have been obscured by tracer diffusion. Input from 50 kHz and 60 kHz (Figs. 9A, 13C) was located more laterally than input from 80 kHz and 90 kHz (Fig. 9C). Both the external nucleus and the pericolicular tegmentum appear to contain labeled cells following WGA-HRP deposits in the superior colliculus (Covey et al., 1987).

The 60 kHz neurons and, to a lesser extent, 50 kHz neurons also projected to a region of densely packed, small cells lateral to the IC and its brachium (Fig. 9A), which Zook and Casseday (1982a) termed the nucleus of the brachium of the inferior colliculus. We distinguish this region, the lateral part of that nucleus (BICNI), from a more rostral area medial to the brachium that contains loosely packed, small and medium-sized cells and that corresponds to Berman's (1968) nucleus of the brachium of the IC in the cat. The medial part also receives ICC input,

moderately from 60 kHz (Fig. 9B) and less so from 80 kHz (Fig. 6A,B), 90 kHz (Fig. 9D), and other frequency bands in ICC.

Other midbrain regions were more weakly labeled. In the contralateral IC, input to the central (Fig. 13A) nucleus was widespread but of low density, while the external nucleus received very few terminals. The superior colliculus received only light, scattered input (Fig. 9B,D).

Among auditory brain stem nuclei, anterograde labeling in HRP, PHA-L, and biocytin experiments was consistent only in the ipsilateral dorsal nucleus of the lateral lemniscus; cochlear and periolivary nuclei were occasionally labeled. In autoradiographic experiments, the cochlear nuclei and the superior olivary complex were virtually unlabeled, while preterminal label in the lateral lemniscal nuclei, the result of tectopontine fibers, obscured any terminal labeling.

Axonal structure

Most axons leaving the IC coursed laterally to join its brachium, and then proceeded ventrally toward the MGB. At the level of the rostral pole of the IC, long dorsoventral segments of brachial axons were contained within 30 μm thick transverse sections (Fig. 10). Their average thickness ranged from $<0.5 \mu\text{m}$ to 3 μm , and two-thirds were between 0.5 μm and 1.5 μm . Some 10% of these axons provided collaterals that passed medially toward the nucleus of the brachium of the IC or the superior colliculus, some clearly terminating in the former nucleus. Thus, single ICC neurons projected to both thalamic and extrathalamic targets.

Axons entering MGB. Tectothalamic axons followed one of three main trajectories: 1) many entered the MGB dorsomedially and passed through the suprageniculate nucleus, the dorsal nucleus, or the medial division; 2) others entered the medial division, coursed ventrally, and then passed laterally into the ventral division; and 3) others remained in the dorsomedial brachium, and then formed compact bundles in the rostral part of the dorsal division while traveling toward the dorsal or rostral pole nuclei.

In VI and Vm, axon terminals had many common features (Figs. 11C, 12A–C). Thus, the terminal plexus was dense and complex, with endings ranging from very small to much larger and knoblike ($> 4 \mu\text{m}^2$). These endings filled an area 20–40 μm in diameter (Figs. 11C, 12B). Many terminal boutons lay in the neuropil, while others abutted somata (Figs. 11C, 12A,C: arrowheads). A few very fine fibers ($< 0.5 \mu\text{m}$) formed en passant swellings at irregular intervals.

Axons in VI from 30–33 kHz arrived either by the dorsomedial (Fig. 12B) or ventromedial trajectories. Most preterminal segments and axonal endings were oriented dorsoventrally and formed fields about 80 μm wide. The sheetlike distribution of the tectothalamic input was consistent with the size and arrangement of the dendritic arborizations in Golgi material (Winer and Wenstrup, 1994b).

In Vm, fibers entered via dorsomedial or medial trajectories. Single fibers and endings labeled by 77–82 kHz or 92–94 kHz deposits formed elongated arcs (Fig. 12C), an arrangement limited to the caudal half of MGB. In contrast to inputs from other frequency bands in Vm or VI, axons and endings labeled by 60–64 kHz deposits did not form a sheet- or arclike pattern, but together filled an area having no obvious laminar organization (Figs. 5B–D, 12A). However, single 60 kHz axons had more highly restricted

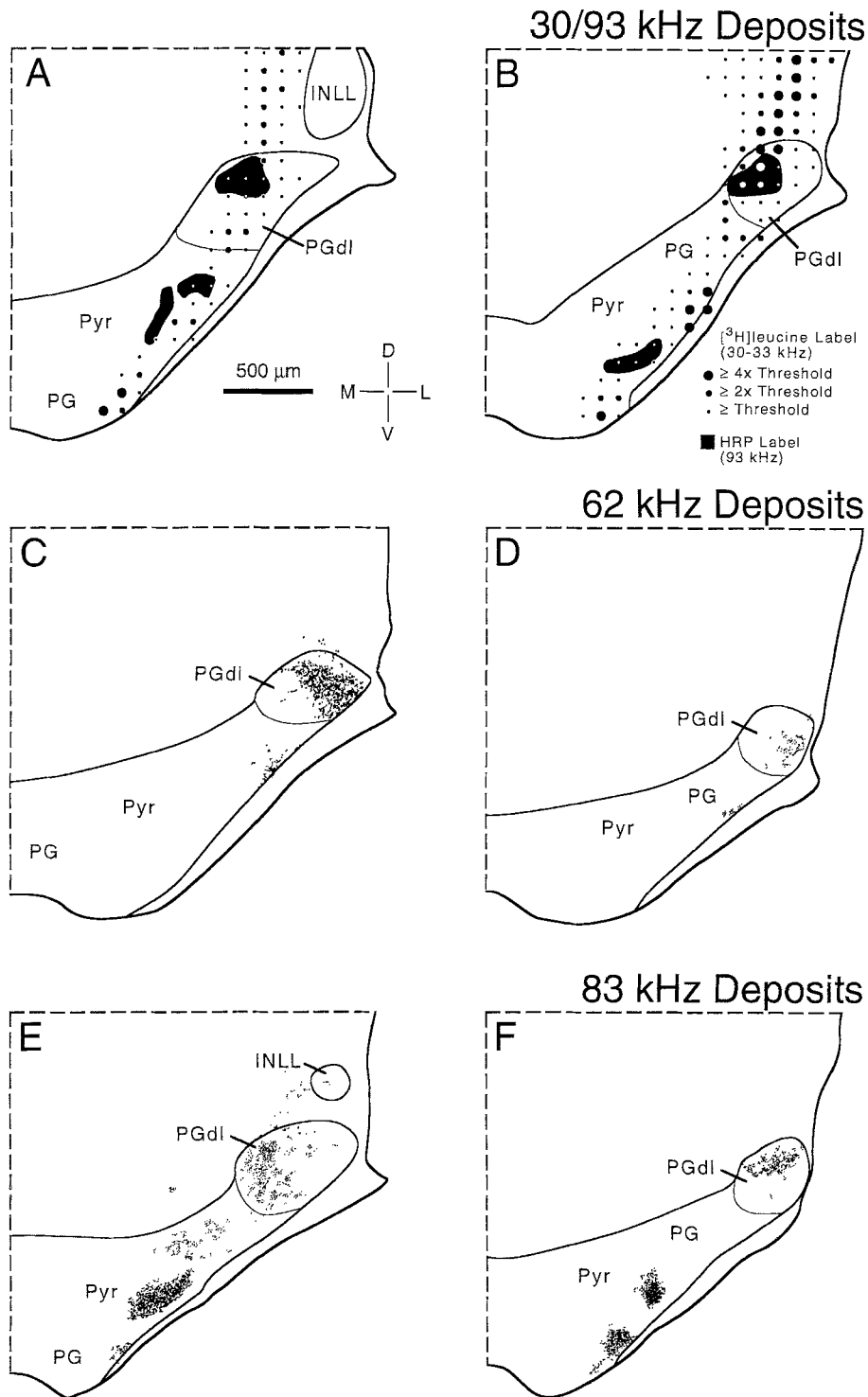


Fig. 8. Anterograde labeling in the ventral pons, located rostral to both the ventral nucleus of the lateral lemniscus and the nucleus of the central acoustic tract. **A,B:** Labeling after three 30 kHz ^3H leucine deposits and four 90 kHz HRP deposits (Table 1, case 987). For 30 kHz, the heaviest presumptive terminal labeling occurred ventrally in the dorsolateral pontine nucleus (PGdl), and in two other pontine loci (PG). Input from 90 kHz terminated medially in the dorsolateral nucleus and in the lateral pontine gray. Inputs from 30 and 90 kHz did not appear to

overlap, although afferent 30 kHz fibers passed through the region of the dorsolateral nucleus labeled by 90 kHz input. **C,D:** Labeling (dots) after 60 kHz HRP deposits (see Fig. 5). Input from 60 kHz terminated in the dorsal and lateral parts of the dorsolateral pontine nucleus, and dorsally in the lateral pontine gray. **E,F:** Labeling (dots) after biocytin deposits at 82 kHz (see Fig. 6), which resembled 90 kHz labeling and terminated medially in the dorsolateral nucleus and ventrally in the lateral pontine gray.

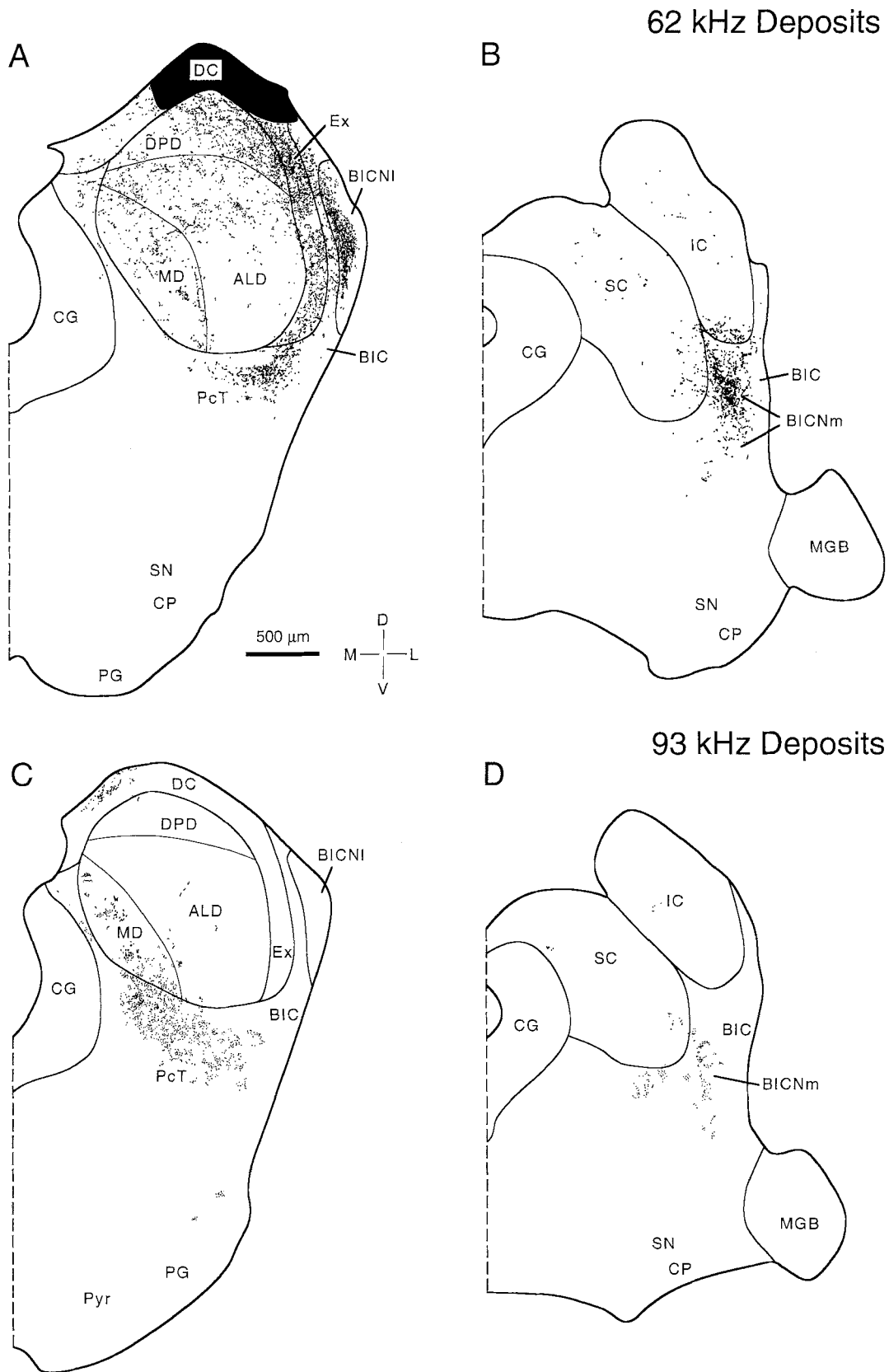


Fig. 9. Anterograde labeling in pericolicular areas. **A,B:** Labeling (dots) after 60 kHz HRP deposits. These sections are successively more rostral than sections in Figure 5G. Terminals in the blackened area in A could not be plotted due to tissue damage. Input from 60 kHz was particularly heavy in the external nucleus (Ex), the lateral and medial parts of the brachium of the inferior colliculus (BICNI and BICNm),

and the pericolicular tegmentum (PcT). **C,D:** Labeling (dots) after 90 kHz HRP deposits (see Fig. 7). These sections are successively more rostral than sections in Figure 7G. Input from 90 kHz terminates mainly in the pericolicular tegmentum, placed more medially than 50 kHz and 60 kHz label.

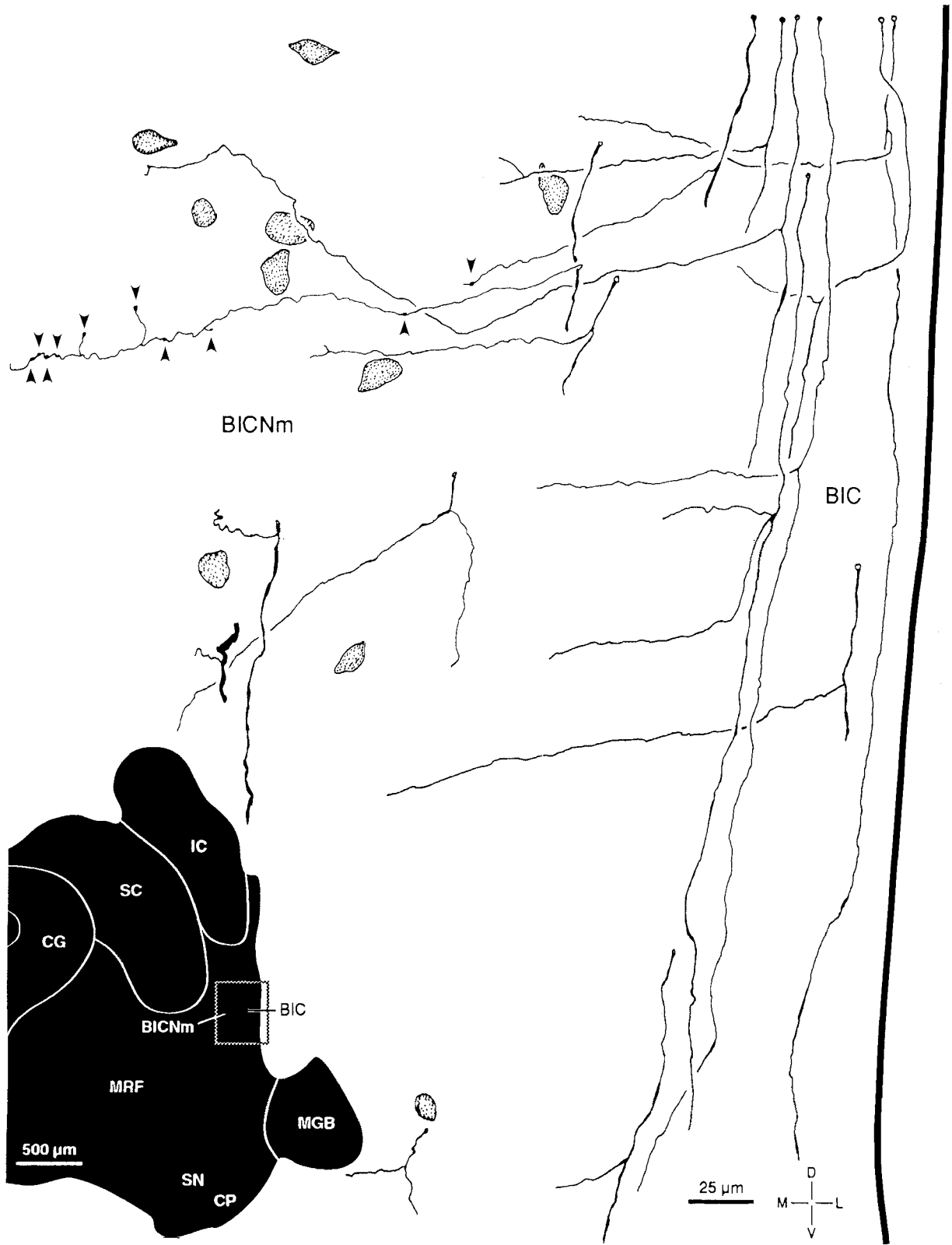


Fig. 10. Branching axons in the brachium of the inferior colliculus, labeled after 60 kHz deposits (see Fig. 5). All branching axons from one section (black figurine) were drawn; about 10% of the axons in this

section were branched. Open circles, transected axons; stippled outlines, neuronal perikarya; arrowheads, location of boutons. Planachromat, N.A. 1.25, $\times 1,875$.

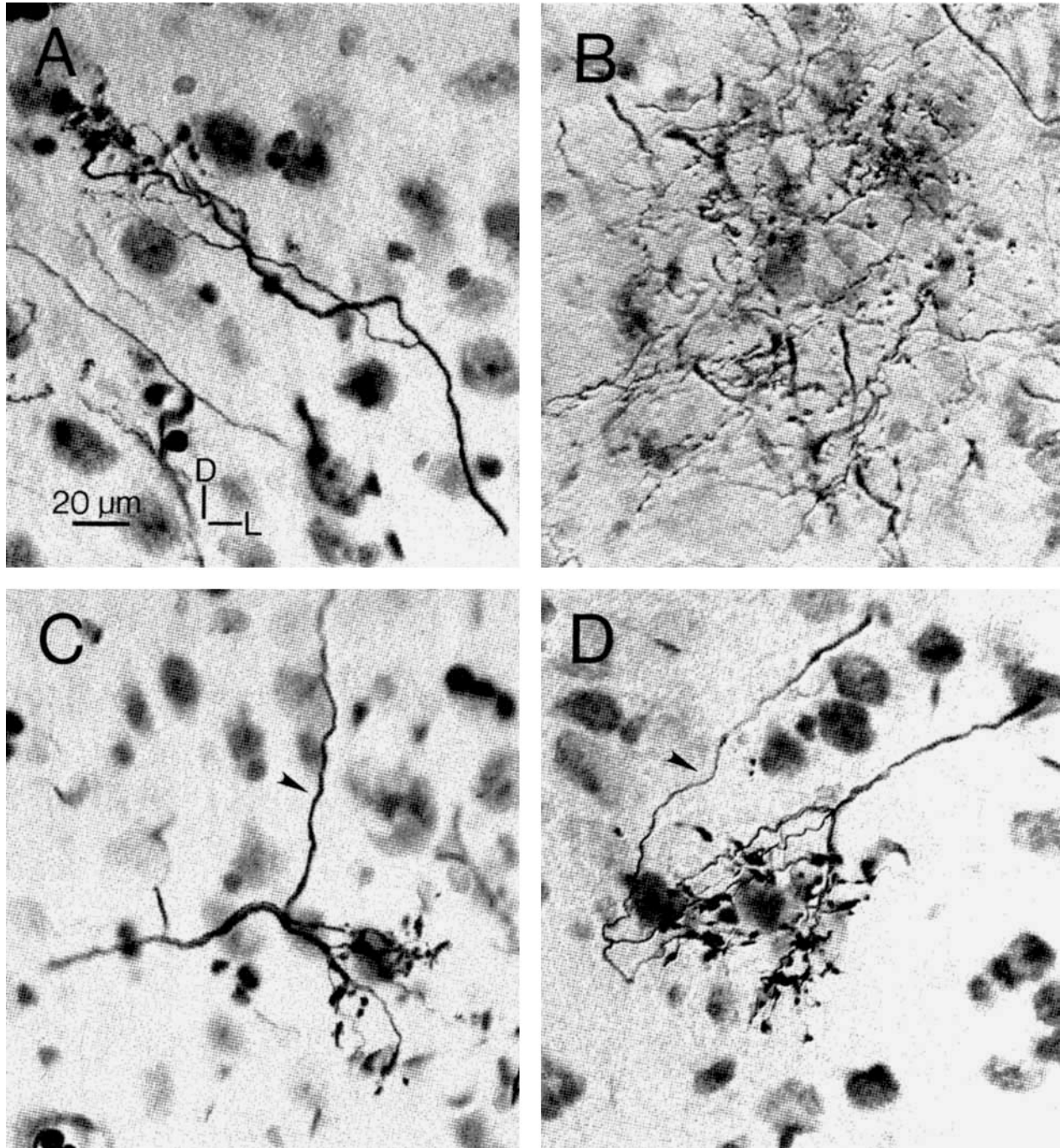


Fig. 11. HRP-labeled tectothalamic axons. **A:** Terminal plexus in the dorsal division labeled by ICC deposits near 62 kHz. Note the restricted domain of the axon as it entered the dorsal division from the underlying ventral division. **B:** Terminal and preterminal plexus in the suprageniculate nucleus, labeled by ICC deposits near 62 kHz. En passant boutons were the prevalent type. **C:** Terminal plexus of an axon in the medial part of the ventral division labeled by ICC deposits near 62 kHz. Note the restricted terminal field. The vertically oriented segment (arrowhead) belongs to another axon. **D:** Terminal plexuses of two

axons in the rostral pole nucleus, labeled by deposits at 30–33 kHz. These may be high frequency fibers damaged in transit through the HRP deposit site. Both the upper axonal segment (arrowhead) and the lower segment have overlapping terminal fields. Rostral pole axons with overlapping terminal fields are also shown in Figure 12D. Protocol for A, C, D: planachromat N.A. 0.65, $\times 625$, differential interference contrast (Nomarski) optics. Protocol for B: planapochromat, N.A. 0.95, $\times 625$, Nomarski optics.

branching patterns than those originating from other ICC different frequency bands.

In the rostral pole and dorsal nuclei of the rostral MGB, the axonal and terminal architecture was significantly

different (Figs. 11D, 12D) from the caudal MGB. Small ($< 0.75 \mu\text{m}$) or medium-sized ($0.75\text{--}2 \mu\text{m}$) axons had many orientations, creating a dense terminal and preterminal plexus. Branching axons, each with several terminal fields,

were more abundant here than in the ventral division (Fig. 12D). The branching pattern may account for the multiple foci of labeling in the dorsal and rostral pole nuclei after 50 kHz (Fig. 4D,E) or 80 kHz deposits (Fig. 6D–F). The most common terminal pattern consisted of complex endings with fine boutons terminating in neuropil and upon somata (Figs. 11D, 12D), although terminal clusters were not as dense as in the ventral division.

Axons entered the dorsal nucleus proper either from a dorsomedial trajectory or through the underlying ventral division (Fig. 11A). Many endings resembled those in the ventral division, with large, complex terminals (Figs. 11A, 12F). Others consisted of string endings with numerous en passant swellings.

The axonal input to the suprageniculate nucleus was distinct (Figs. 11B, 12E). Many medium-sized brachial fibers coursed ventrolaterally, and both medium and small caliber fibers branched off the main axon trunk (Fig. 12E, 4–6) and entered the neuropil, giving rise to many en passant swellings. These fine axonal segments often traveled at right angles to the trajectories of the larger axons transiting the nucleus, imparting a distinctive appearance to the fiber architecture. Many boutons lay near primary dendrites of the principal neurons, well-situated to make synaptic contacts along them.

Extrathalamic axons. Distinctive axonal and terminal patterns were likewise evident in the extrathalamic targets. One pattern was common in the contralateral ICC (Fig. 13A). Over half of the axons passing through the commissure of the IC and all preterminal axons in the contralateral ICC were very fine ($\leq 0.5 \mu\text{m}$). Both en passant and terminal clusters of small boutons occurred. For a single axon, the density of boutons could exceed $1/3 \mu\text{m}$. However, the overall density of terminals in the contralateral ICC was lower than in other extrathalamic targets.

In the external nucleus of the IC and the subcollicular tegmentum (Fig. 13C), en passant and simple terminal swellings were interspersed with tectothalamic axons of varied sizes. The density of boutons could be high, even in tegmental regions of low neuronal density (Fig. 9A,C). Bouton size varied more than in the contralateral ICC, and some endings were more complex. Some axonal segments were collaterals of larger fibers entering the brachium of the inferior colliculus (Fig. 13C, arrowhead). Comparable boutons occurred in the nucleus of the brachium of the IC, with en passant and simple terminal endings of different sizes predominating. Many axons entering this region were collaterals of brachial fibers descending toward the MGB (Fig. 10).

The ICC afferents to the pretectum were as distinctive in form as in their high density (Fig. 13B). Among the relatively few neurons lay a dense plexus of axons having varied thickness and orientation. En passant and simple boutons were abundant, but their targets were obscured by the dense axonal network; these included some axosomatic endings, although most were in neuropil.

The dorsolateral pontine nucleus presented still another axonal pattern (Fig. 13D). Among densely packed large cells, predominantly medium-sized axons descended from ICC. Terminals were more varied than in other extrathalamic targets. Both complex, knoblike endings and simple terminal and en passant boutons occurred. Perisomatic endings were common, suggesting that single collicular efferents could strongly affect the firing of individual pontine neurons. Figure 13D shows the axonal architecture

in a region with fewer axons; fibers and terminals were much denser at the center of the terminal field.

DISCUSSION

This study demonstrates that the central nucleus of the inferior colliculus in the mustached bat projects widely to the pons, midbrain, and thalamus (Table 2). In the MGB alone are three major targets, with several extrathalamic projections to the pontine gray, pretectum, and pericolicular region. Moreover, the outputs of the ICC are highly diverse, differing in constituent frequency bands, organization, or axonal morphology. These anatomically diverse projections must generate diverse physiological properties within target nuclei, contributing to functional circuits that analyze different biosonar components or that direct auditory information to different premotor control centers. ICC neurons are thus one synapse removed from several indirect targets, including the cerebellum, superior colliculus, and cerebral cortex, which may control sonar-guided navigation and prey-catching as well as responses to other acoustic signals.

ICC inputs to MGB

The ICC in the mustached bat projects exclusively to the ipsilateral MGB, similar to the horseshoe bat (Schweizer, 1981) but different from other mammals (e.g., cat and tree shrew), which have a weaker contralateral projection (Kudo and Niimi, 1978; Oliver and Hall, 1978; Andersen et al., 1980; Rouiller and de Ribaupierre, 1985). The ICC targets the ventral and medial divisions, as in other mammals, (Oliver and Hall, 1978; Andersen et al., 1980; Kudo and Niimi, 1980; Calford and Aitkin, 1983; LeDoux et al., 1985; Winer, 1992), but also projects strongly to the dorsal nucleus, the suprageniculate nucleus, and the rostral pole (Fig. 14). These latter projections appear to be novel, and some may represent pathways specialized for the analysis of biosonar information. Below we consider each ICC-MGB input pattern and its implications for MGB organization and function.

Topographic projection to the ventral division. Across the ventral division, there is a tonotopic input pattern from ICC, best visualized about 40–45% through the caudal-to-rostral dimension of the MGB (Fig. 14A). Low frequencies project laterally and higher frequencies project to more medial and rostral loci. V1 receives input from frequencies below 60 kHz; 25–33 kHz input terminates more laterally than does 50–59 kHz input (Fig. 14A–C). Vm receives higher frequency input, beginning most caudally with projections from the specialized 60 kHz region in ICC. More rostrally, 60 kHz input assumes a more lateral and dorsal location as it is displaced by higher frequency input (80 kHz and 90 kHz) located more medially (Fig. 14A). It is presumed that the projections of ICC frequency bands not tested here fit within the tonotopic arrangement described in Figure 14. For example, frequencies in the 10–24 kHz range may project most laterally in V1, while frequencies above 94 kHz may terminate in the most medial part of Vm.

The present data closely agree with Olsen's (1986) physiological studies, in which pure tone responses were confined mostly to the caudal half of the MGB, and best frequencies were arranged in a more or less lateral-to-medial, low-to-high frequency pattern. In retrograde transport studies, Olsen (1986) showed that V1 and Vm provide the major input to the tonotopically organized field in primary audi-

tory cortex. The frequency representation in AI (Suga and Jen, 1976) displays features that agree closely with the tonotopic organization implied by the pattern of collicular input to the ventral division. Thus, the 60 kHz representation is quite large, while the representations of frequencies in the FM₂ and FM₃ sonar components are, at best, very small.

The tonotopic pattern and arrangement of ICC axons and terminals also correspond well with the arrangement of principal cell dendrites in Golgi-impregnated neurons (Winer and Wenstrup, 1994b). Thus, labeling in VI, whether preterminal axon segments or dense clusters of terminals, assumes a dorsoventral orientation, often forming bands. Dendritic laminae also assume a dorsoventral orientation, aligning them with incoming axons and their terminal boutons. Similarly, 80 kHz and 90 kHz inputs to the medial part of Vm form restricted bands or arcs that correspond to dendritic laminae in this region. The pattern of 60 kHz input to Vm is an exception; these axons do not form bands or arcs, but assume a patchlike character. However, this arrangement agrees well with the Golgi studies, because the region labeled by 60 kHz deposits does not show a laminar dendritic organization [see Figs. 1 and 2 in Winer and Wenstrup (1994b)]. In the ICC as in the MGB, the neuronal architecture within the 60 kHz representation differs from the laminar architecture in regions representing both higher and lower frequencies (Zook et al., 1985).

Although the ventral division probably analyzes both sonar and nonsonar acoustic signals across its tonotopic range, two noteworthy features of the ICC's tonotopic projection bear on the analysis of sonar echoes by ventral division neurons. First, 60 kHz (CF₂) input to the ventral division is extensive, preserving the disproportionately large representation in the cochlea (Kössl and Vater, 1985; Zook and Leake, 1989) and the ICC (Zook et al., 1985; O'Neill et al., 1989). A major function of specialized 60 kHz neurons is believed to be the representation of insect wingbeat patterns, encoded by the response of CF₂ neurons to periodic amplitude and frequency modulations in echoes. Sensitivity to the behaviorally relevant modulation patterns is common among 60 kHz ICC neurons (Bodenhamer and Pollak, 1983; Lesser, 1988; Lesser et al., 1990), and it is likely that many project to the ventral division of MGB. How modulation sensitivity is distributed throughout the 60 kHz representation of MGB is not known.

The large 60 kHz representation in the ventral division is also likely to encode sound localization cues. In the ICC, 60 kHz binaural inhibitory neurons (EI neurons) are segregated from other binaural and monaural neurons, and their sensitivity to interaural intensity differences is topographically organized (Wenstrup et al., 1986). These neurons project to the ventral division, and preliminary evidence indicates that 60 kHz EI neurons project differently than do monaural neurons (Wenstrup, 1992a). Thus, some isofrequency representations in MGB, such as the 60 kHz representation, may contain functional subdivisions analyzing different acoustic features. A similar conclusion has been suggested by previous work in cats (Middlebrooks and Zook, 1983).

These considerations suggest that much of the ascending information concerning CF₂ echoes projects through the ventral division. This contrasts sharply with frequency bands representing FM components of the echo. Thus, the second noteworthy feature of the tonotopic projection is that there are only small inputs from 48–60 kHz and 72–90

kHz, the frequency bands associated with the FM₂ and FM₃ components of the sonar signal. Since these are well represented in the ICC (O'Neill et al., 1989; this study), their modest contributions to the tonotopic input to the ventral division indicate a significant departure from the pattern established in the cochlea and preserved in the ICC (Frisina et al., 1989; this study).

The main MGB projection from FM₂ and FM₃ representations in ICC is to the rostral MGB, where specialized neurons respond to the delay between echo components, thereby encoding target distance (see next section). Does this strong projection outside the tonotopic axis preclude their participation in analyses performed within the tonotopic axis? One question concerns the representation of target elevation and azimuth. In ICC, target location information is preserved in the binaural responses of neurons tuned to a range of echo frequencies (Fuzessery and Pollak, 1985; Wenstrup et al., 1988b; Fuzessery et al., 1990). The reduced FM₂ and FM₃ input to the ventral division suggests that these frequencies may not contribute to azimuthal and elevational localization. Thus, it remains to be determined what information is conveyed by these frequency bands within the tonotopic pathway.

Projection to the rostral MGB. The distinctive ICC input to the rostral one-half of the MGB may contribute to neural circuits specialized for the analysis of biosonar or other species-specific acoustic signals (Fig. 14B,C). Targeting the rostral pole nucleus, the dorsal nucleus, and the medial division to a lesser extent, this projection includes all frequency bands tested. The input is frequency-specific but not tonotopic, that is, each frequency band displays a characteristic distribution, but inputs do not form a tonotopic sequence. For example, in the middle one-third of the MGB, projections from CF₂ and CF₃ frequencies are closely apposed in the rostral pole and dorsal nuclei, but these frequency bands send little input to the rostral third of MGB. There, ICC input is dominated by FM₂ and FM₃ (and possibly FM₄) frequency bands (Frisina et al., 1989; this study). Each provides large, dense, apparently interdigitating patches of input to the rostral pole and/or the dorsal nuclei. Thus, in parts of the rostral MGB, the frequency organization is not cochleotopic, but may instead be based

Fig. 12. (See overleaf.) Architecture of ICC axons in MGB subdivisions. See key in black in Figure 13; approximate location indicated by black letters on white circles. **A:** Labeling in the medial part of the ventral division after ICC deposits near 62 kHz. Boutons ended both in neuropil and near perikarya (arrowheads). **B:** Labeling in the lateral part of the ventral division after 30–33 kHz deposits. Axons and terminals formed an arc recapitulating the arrangement of principal cell dendrites in Golgi material (Winer and Wenstrup, 1994b). No perikarya were visible in this unstained section. Heavy curved line, dorsolateral surface of MGB. **C:** Labeling in the medial part of the ventral division after 93 kHz deposits. Boutons ended both in neuropil and near perikarya (arrowheads). **D:** Labeling in the rostral pole nucleus after 77–82 kHz deposits. Many axons (1–3) formed two branches separated by at least 100 μ m. Two axons, (1 and 2), entered ventrolaterally, and each had two separate terminal plexuses that were nearly congruent. Note prominent axosomatic endings. **E:** Labeling in the supragenulate nucleus after 62 kHz deposits. Several axons branched in the supragenulate nucleus (4–6). Some (4) sent collaterals into the supragenulate while the main trunk proceeded to the ventral division. **F:** Labeling in the dorsal nucleus after 62 kHz deposits. Boutons were similar to those in the medial part of the ventral division in this experiment (A). All sections are from HRP experiments and processed using heavy metal-DAB as chromogen. Protocol for all drawings: planachromat, N.A. 1.25, $\times 1,875$.

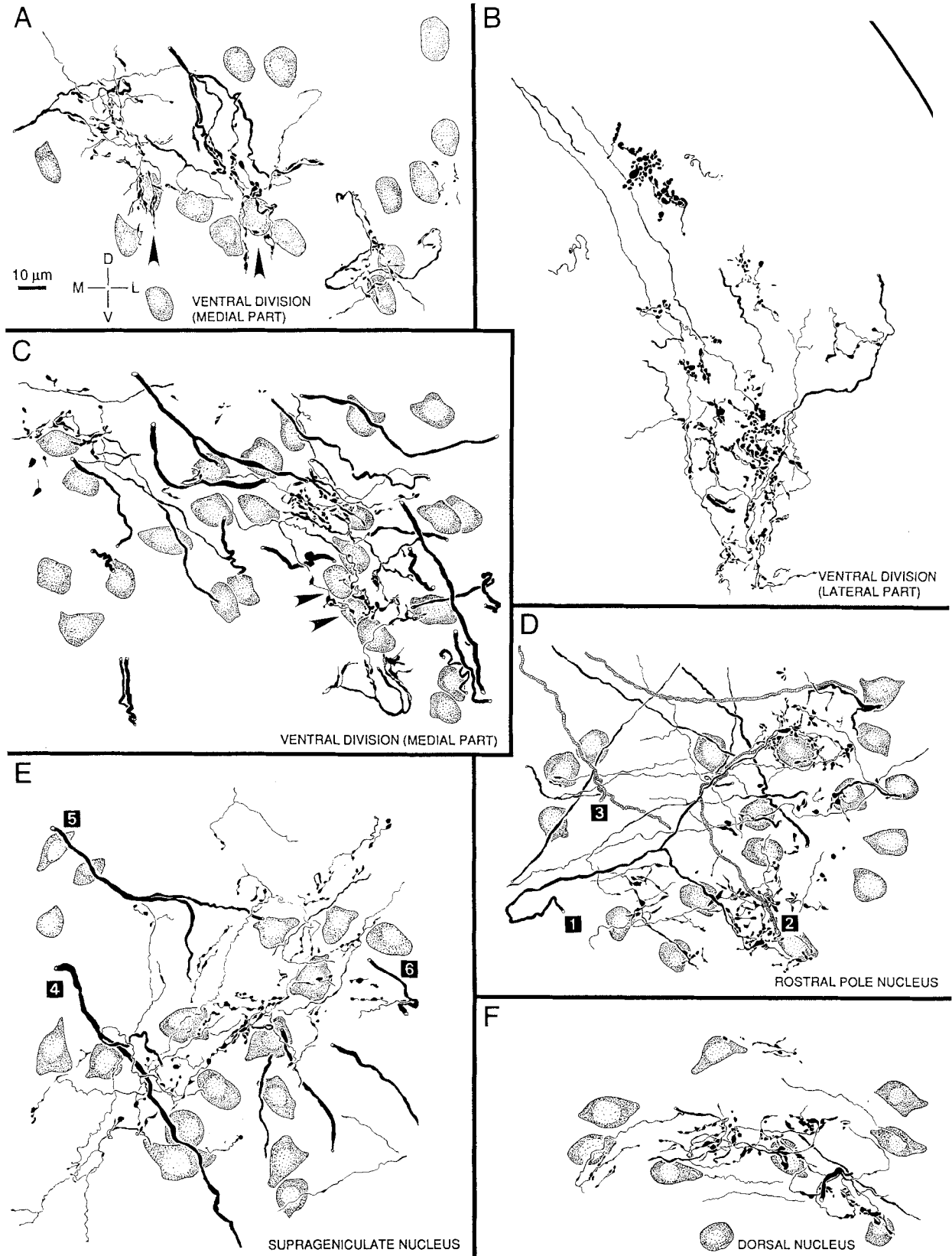


Figure 12 (See legend on previous page.)

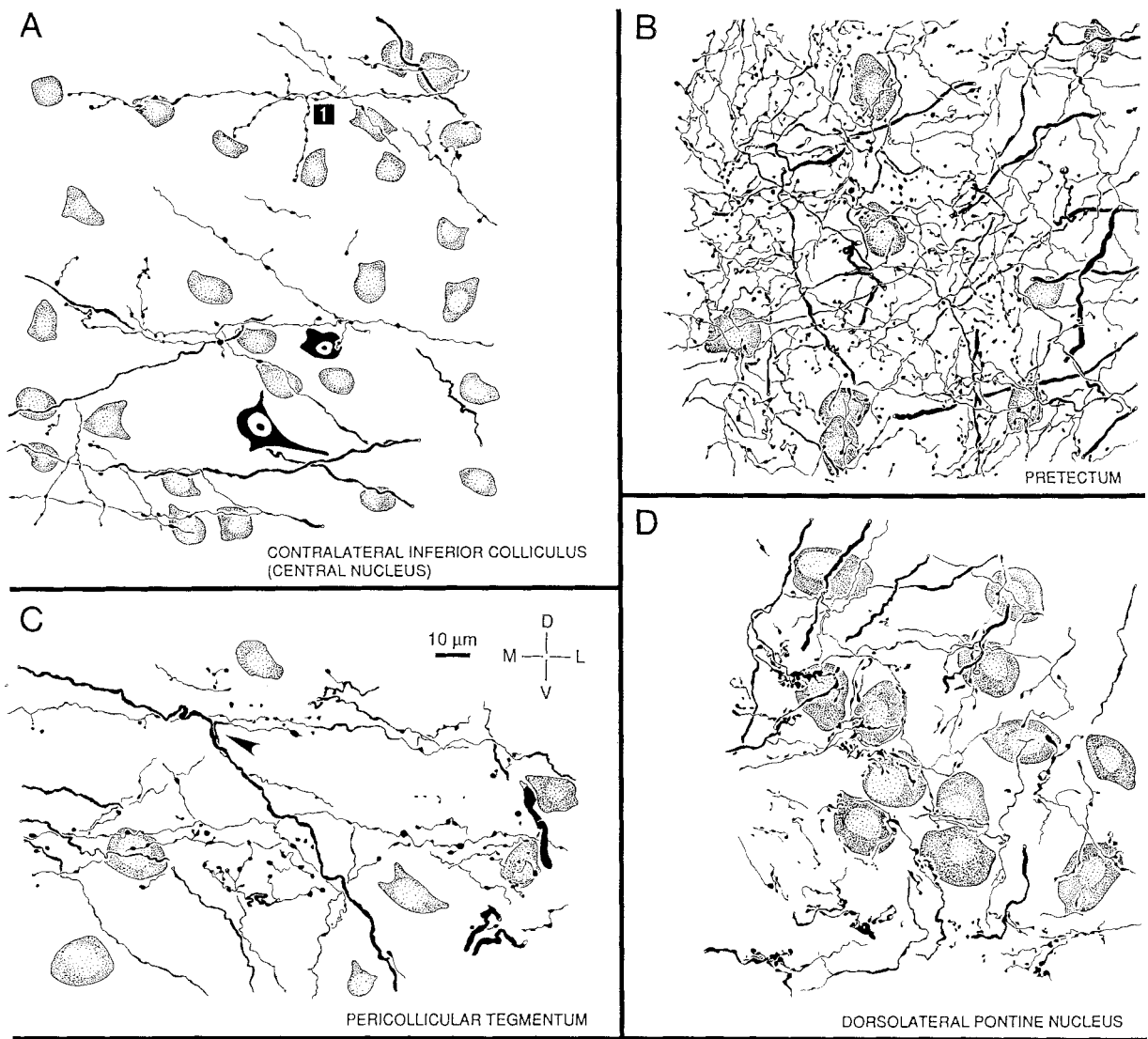


Fig. 13. Architecture of ICC axons in extrathalamic targets. See key in black; approximate location indicated by black letters on white squares. **A:** Labeling in the contralateral ICC after 62 kHz deposits. Blackened cells were retrogradely labeled. Some axons had large numbers of boutons (1), but the overall density of labeled boutons was low. Mediolateral orientation is reversed in this contralateral section; the midline is to the right. **B:** Labeling in the pretectum after 77–82 kHz deposits. Pretectal label in 80 kHz experiments was the densest seen in this study. **C:** Labeling in the pericollicular tegmentum after

deposits near 62 kHz. This label was similar in form and continuous with label in the external nucleus of the inferior colliculus. Arrowhead, collateral of brachial axon terminating in pericollicular tegmentum. **D:** Labeling in the dorsolateral nucleus of the pontine gray after deposits near 62 kHz. Note perisomatic labeling. This drawing was made away from the densest labeling in order to resolve individual axons better. All sections are from HRP experiments and were processed using heavy metal-DAB as chromogen. Protocol as in Figure 12.

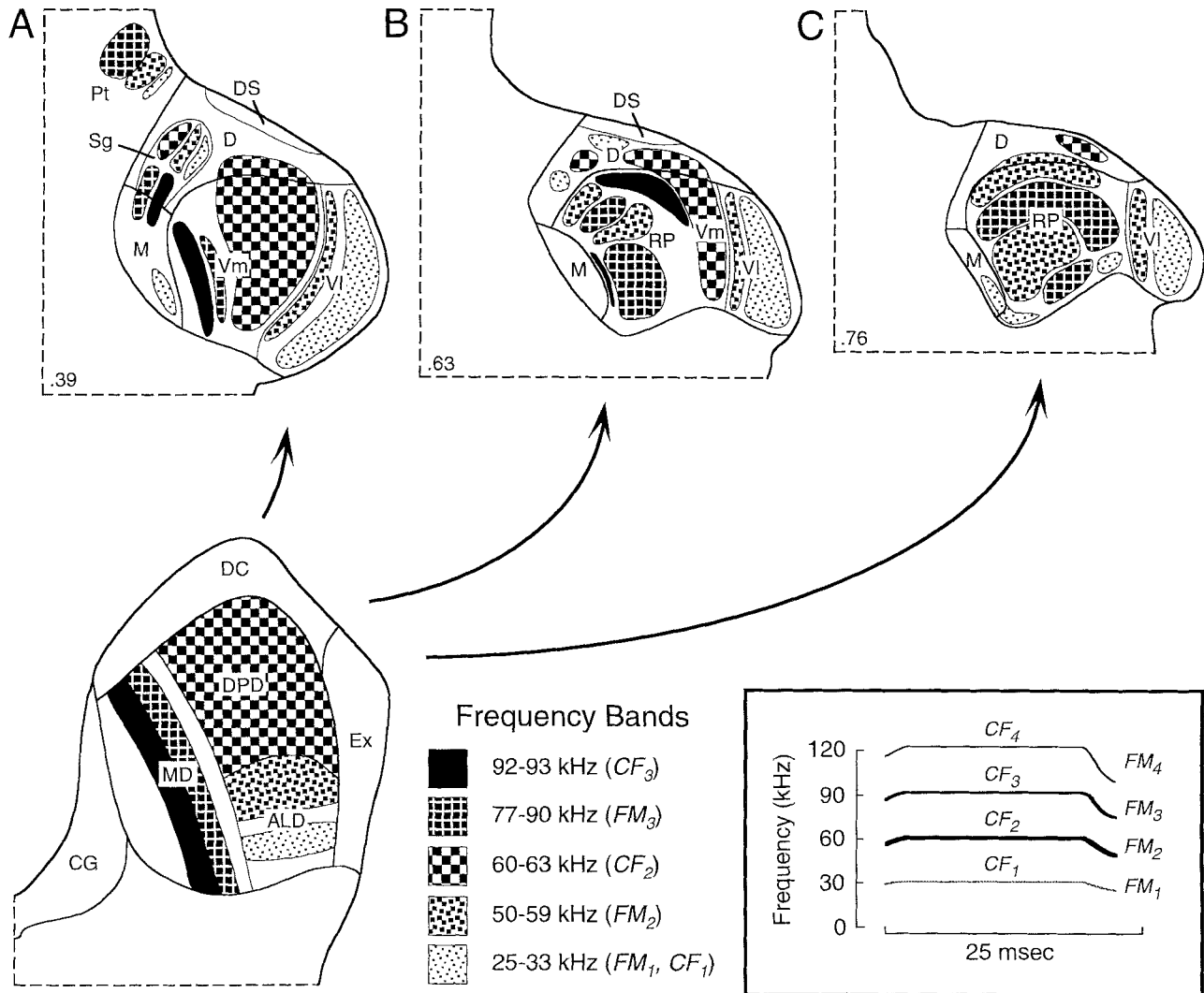


Fig. 14. Schematic summary of the distribution of inputs to MGB (A-C) from five ICC frequency bands that analyze major elements of the bat's sonar signal. Three major projection systems are described in the text. One terminated in the lateral (VI) and medial (Vm) parts of the ventral division and was tonotopically organized (A and parts of B, C). A second terminated in the suprageniculate nucleus (Sg) and was also tonotopic (A). A third set of projections was found principally in the

rostral pole (RP) and dorsal (D) nuclei (B, C). These inputs may be organized according to functional biosonar components; ICC frequency bands representing CF_2 and CF_3 components terminated at middle MGB levels (B), while FM_2 and FM_3 projections were extensive and ended well into the most rostral part of MGB (B, C). Note also projections from FM frequency bands terminating in the region of the pretectum (A).

on the functional properties of biosonar components represented within specific frequency bands.

The rostral MGB is dominated by combination-sensitive neurons, cells that display a facilitated response to two spectrally distinct signals (Olsen, 1986; Olsen and Suga, 1991a,b). These are thought to be specialized for responding to combinations of specific components in the sonar pulse and echo. Combination-sensitive neurons have been well described in areas of the auditory cortex outside AI (O'Neill and Suga, 1982; Suga et al., 1983; Suga and Horikawa, 1986), and most MGB neurons projecting to cortical combination-sensitive areas are located in its rostral half (Olsen, 1986). Because similar neurons have not been found in the IC (O'Neill, 1985), it is believed that combination-sensitive responses are constructed in the MGB (Olsen, 1986; Olsen and Suga, 1991b).

Two classes of combination-sensitive neuron have been described. CF/CF neurons respond best to combinations of the CF_1 component in the sonar pulse and a higher harmonic CF component (near 60, 90, or 120 kHz) in the echo, with the frequencies of the two components being a critical stimulus feature. CF/CF neurons are believed to encode the velocity of sonar targets (Suga et al., 1983). In MGB, such neurons are found mainly in the middle third of MGB (Olsen and Suga, 1991a), corresponding to the 60 and 90 kHz ICC input observed in the present study.

The second class, FM-FM neurons, responds best to combinations of the FM_1 component in the pulse and a higher harmonic FM in the echo; the timing of the two components is the critical stimulus feature here. FM-FM neurons, topographically ordered in cortex according to their delay sensitivity, are believed to encode the range of

sonar targets (O'Neill and Suga, 1982; Suga et al., 1983). Chemical inactivation of a cortical FM-FM area disrupts a temporal (delay) discrimination task (Riquimaroux et al., 1991). In the MGB, FM-FM neurons are recorded primarily in the rostral third—our rostral pole and dorsal nuclei—the region that receives heavy input from FM₂ and FM₃ representations in ICC. Different types of FM-FM neurons, (e.g., FM₁-FM₂ or FM₁-FM₃) have a patchy organization in the rostral MGB (Olsen, 1986), and this physiological organization corresponds well to the interdigitating arrangement of FM₂ and FM₃ inputs from the ICC. Because FM₁-FM₄ neurons have also been recorded in the rostral MGB (Olsen and Suga, 1991b), additional ICC inputs probably originate from 96–120 kHz, the frequencies in the FM₄ sonar component.

Combination-sensitive neurons require input from frequency bands representing either FM₁ or CF₁ sonar components, as well as from higher frequency components. We thus expected to find significant overlap between FM₁ or CF₁ inputs and input from higher frequency ICC regions, but none was apparent. However, the present study was not designed to assess overlap directly, and we cannot exclude the possibility that our low frequency tracer deposits missed a part of the FM₁ and CF₁ representations. Additional studies are clearly required. Preliminary results from experiments using dual anterograde tracers (Wenstrup, 1992b) are consistent with the present findings, and suggest that low frequency input to combination-sensitive regions in the MGB does not arrive directly from the ICC.

Projection to the suprageniculate nucleus. The strong ICC input to the suprageniculate nucleus contrasts sharply with results in the cat (Andersen et al., 1980; Kudo and Niimi, 1980; Calford, 1983) and rat (LeDoux et al., 1985), in which no ICC projection is evident. Every ICC frequency band that was tested contributes to this projection, and the projection was roughly topographic (Fig. 14A). It is unclear, however, whether the topographic input pattern confers a physiological tonotopy onto this nucleus, since the principal neurons have large, radiating dendritic fields that overlap, each filling a significant part of the nucleus (Winer and Wenstrup, 1994b). The suprageniculate nucleus also receives substantial input from the nucleus of the central acoustic tract and the external nucleus of the IC (Casseday et al., 1989), and the extent to which these and ICC inputs are aligned by frequency is not known. Thus, suprageniculate neurons may receive input from several frequency representations, and might therefore show broad frequency tuning, as they do in the cat (Calford, 1983).

The function of auditory pathways through the suprageniculate nucleus is obscure. In both the mustached bat (Kobler et al., 1987) and the rat (Kurokawa et al., 1990), it projects to auditory and frontal cortical areas. In the mustached bat, the frontal cortical target displays robust auditory responses and projects strongly to the superior colliculus (Kobler et al., 1987); it may contribute to acoustic orienting responses coordinated by the superior colliculus. In rats, the suprageniculate nucleus and the medial division of MGB project to regions of the amygdala that mediate learned emotional responses to sounds (LeDoux et al., 1985, 1986). The existence of this pathway in the mustached bat is not known, but one might expect a high degree of auditory-limbic interaction in an animal that depends so heavily on sound to perceive its environment and communicate with conspecifics.

Organization of MGB and relation to other species.

The present study supports an architectonic plan based on neuronal, cyto-, and myeloarchitecture as well as on chemical anatomy (Winer et al., 1992; Winer and Wenstrup, 1994a,b). In the ventral division, for example, a tonotopic projection pattern corresponds to a region characterized by a fibrodendritic laminar arrangement. In the suprageniculate nucleus, defined by its large cells, their radiate dendritic branching, and the distinct pattern of GABAergic terminals, the structure and organization of ICC axons serve to distinguish it further from adjacent nuclei. The rostral pole nucleus, distinguished from the ventral division by its cyto- and myeloarchitecture (Winer and Wenstrup, 1994a), also differs in tectothalamic projections: in the branching pattern of ICC axons and in the nontopographic organization of ICC inputs.

MGB subdivisions in the mustached bat differ in the degree of their correspondence to subdivisions described in other mammals. The ventral division has the strongest anatomical and physiological parallels. In all mammals, the ventral division maintains frequency-specific processing of acoustic information by means of sharply tuned, tonotopically organized neurons that respond reliably and with temporal fidelity to tonal signals (Aitkin and Webster, 1972; Rouiller et al., 1979; Calford, 1983; Rodrigues-Dagauff et al., 1989; Clarey et al., 1992). In the cat's ventral division, the best known, there is a roughly lateral-to-medial, low-to-high frequency tuning gradient (Rose and Woolsey, 1949; Aitkin and Webster, 1972; Calford and Webster, 1981; Imig and Morel, 1985). In the mustached bat's VI (Winer and Wenstrup, 1994b), as in the cat (Morest, 1964; Winer, 1985, 1991, 1992), isofrequency contours (Olsen, 1986) correspond well to the fibrodendritic laminae described in Golgi material. However, in Vm, the tonotopic sequence and the arrangement of axons and dendrites are distorted by the massive 60 kHz representation, and their relation to the coiled laminae in the *pars ovoidea* of the cat's ventral division (Morest, 1965; Winer, 1985) is uncertain.

Similarities extend to the structure of tectothalamic axons and terminals. Originating from physiologically defined subdivisions in ICC and ending in the mustached bat's ventral division, these resemble the form and arrangement of brachial axons entering the MGB of the cat (Morest, 1965; Majorossy and Rethelyi, 1968; Jones and Rockel, 1971). Terminals, including complex arrays of large, knob-like swellings, are densely distributed in the ventral division, most ending on perikarya or primary dendrites (Morest, 1965; Majorossy and Kiss, 1976). Similar patterns of terminals have been described among individual HRP-filled brachial axons in the ferret (Pallas et al., 1991). These parallels suggest that the lemniscal component of the auditory tectothalamocortical pathway is the most highly conserved in the mustached bat.

The degree of correspondence is somewhat less in the suprageniculate nucleus, where architectonic similarities to other mammals exist in parallel with differences in connectivity. For example, ICC boutons in the suprageniculate nucleus differ from those elsewhere in the MGB, consisting primarily of en passant endings. This architecture corresponds well to that described in Golgi studies of the cat's MGB (Winer and Morest, 1984). However, the difference in inputs is striking; there are no projections from ICC in the cat (Andersen et al., 1980; Kudo and Niimi, 1980; Calford, 1983) or the rat (LeDoux et al., 1985). Physiological similarities to the cat (Calford, 1983) may include broad tuning.

TABLE 2. Summary of Major Targets of ICC Projections in the Mustached Bat

Target	Spectral contribution	Organization of ICC inputs	Some documented or possible targets
MGB nuclei			
Ventral division	All frequencies	Tonotopic	Primary auditory cortex ¹
Rostral MGB	All frequencies	Functional sonar components	FM-FM, CF/CF areas of auditory cortex ¹
Suprageniculate nucleus	All frequencies	Tonotopic	Auditory cortex, frontal cortex ²
Midbrain nuclei			
Pretectum	FM frequencies	Patchy	Pontine nuclei ^{3,4}
External nucleus of ICC	60 kHz, weak 50 kHz	Unknown	Superior colliculus, ⁵ pretectum, ⁶ MGB ⁷⁻¹⁰
Pericollicular tegmentum	> 30 kHz	Weakly tonotopic	Superior colliculus ⁵
Nucleus of the brachium of IC, lateral part	50-60 kHz	Unknown	Unknown
Nucleus of the brachium of IC, medial part	All frequencies	Unknown	Pretectum, superior colliculus, MGB ¹¹
Pontine nuclei			
Dorsolateral nucleus	All frequencies	Patchy	Contralateral cerebellum ¹²
Lateral and ventral areas	All frequencies	Patchy	Contralateral cerebellum ¹²

¹Olsen, 1986.²Kobler et al., 1987.³Aas, 1989; in the cat.⁴Mihailoff et al., 1989; in the rat.⁵Covey et al., 1987.⁶Kudo et al., 1983; in the cat.⁷Oliver and Hall, 1978; in the tree shrew.⁸Kudo et al., 1980; in the cat.⁹Calford and Aitkin, 1983; in the cat.¹⁰LeDoux et al., 1985; in the rat.¹¹Kudo et al., 1984; in the cat.¹²Schuller et al., 1991; in the horseshoe bat.

However, some suprageniculate neurons in the mustached bat (Casseday et al., 1989) have shorter latencies than in the cat (Calford, 1983), probably due to the strong, short-latency input from the ICC or nucleus of the central acoustic tract. These observations suggest that the organization, connections, and function of suprageniculate neurons may show species-specific variations.

The affiliation of the rostral MGB, especially the rostral pole nucleus, remains a puzzle (Winer and Wenstrup, 1994a). Others have identified combination-sensitive regions of the rostral MGB as the deep dorsal nucleus (Olsen, 1986; Olsen and Suga, 1991a), and the reception of high frequency ICC input corresponds to the deep dorsal nucleus in the cat (Andersen et al., 1980; Calford and Aitkin, 1983; Rouiller and de Ribaupierre, 1985). However, our studies reveal no clear counterpart to other mammals, and the known physiological responses and cortical connections of this region (Olsen, 1986; Olsen and Suga, 1991a,b) suggest specializations related to the bat's sonar behavior. Still, the rostral MGB is generally less understood in all species (Winer, 1992), and further study may reveal parallels to the mustached bat.

Extrathalamic projections of ICC

Projections to the pretectum. One of the most intriguing extrathalamic targets of the ICC is an area dorsomedial to MGB that we have provisionally assigned to the pretectum. Although the pretectum is best known for its role in visuomotor reflexes, it also receives somatosensory (Berkley and Mash, 1978; Wiberg et al., 1986; Yoshida et al., 1992) and auditory inputs (Kudo et al., 1983, 1984),

particularly to the anterior pretectal nucleus. In cats, much of the auditory projection to the pretectum originates in midbrain regions adjoining the ICC, but not from ICC itself, and terminates in the anterior pretectum and adjacent midbrain reticular formation (Kudo et al., 1983, 1984). In the mustached bat, an apparently corresponding area receives strong input from the ICC, perhaps reflecting this animal's high reliance on acousticomotor responses.

The intriguing aspect of these results is the strength and frequency specificity of the ICC input (Fig. 14A). Indeed, this region received the densest input of any target in our survey, and it arose from the ICC representations of FM components in the echolocation signal [50 and 80 kHz; this study and Frisina et al. (1989)]. Projections from the FM₄ representation in ICC are also very strong (Wenstrup, unpublished observations). Input from the frequencies in the fundamental sonar component also terminate here, but 60 kHz and 90 kHz projections are very weak. These inputs suggest that this region relays or analyzes target distance information conveyed by the FM sweep, and this conclusion is reinforced by Olsen's (1986) observation that a cortical area containing FM-FM delay-sensitive neurons also projects to the pretectum. Such information may be furnished to a variety of premotor centers coordinating prey capture, including vocalization centers, which increase the sonar pulse rate as a bat's distance to its prey decreases. Additional connections and functional properties of the mustached bat's pretectum are unknown, but one target in other species is the precerebellar pontine gray (Aas, 1989; Mihailoff et al., 1989).

Projections to the pontine gray. The ICC projects strongly to the cell masses of the ventral pons. Each ICC frequency band examined projects to two or more targets in the pontine gray: one in the dorsolateral nucleus, one in the lateral pontine area, and often a third in either the lateral or ventral area. ICC input is patchy, forming dense, highly restricted terminal zones. Although it is uncertain whether projections from adjacent frequency bands overlap, the topography of inputs suggests that physiological recordings should find small patches of similarly tuned neurons, without a clear tonotopic arrangement. Physiological studies in the horseshoe bat (Schuller et al., 1991) and the big brown bat (Kamada et al., 1992) confirm this.

What distinguishes bats from other mammalian groups, at least on the basis of present evidence, is that strong ICC input occurs only in bats (Schweizer, 1981; Frisina et al., 1989; Schuller et al., 1991). It is modest (Andersen et al., 1980; Hashikawa, 1983) or absent (Aas, 1989; Mihailoff et al., 1989) in other species. Although other auditory centers project to the pontine grey in bats (Olsen, 1986; Schuller et al., 1991) and other mammals (Kawamura and Chiba, 1979; Hashikawa, 1983; Azizi et al., 1985; Aas, 1989), the strong ICC input exclusive to bats suggests that auditory pontine neurons and their targets in the cerebellum serve a more specialized, biosonar-related role. Indeed, cerebellar auditory neurons in the mustached bat respond predominantly to biosonar frequencies (Jen et al., 1982; Horikawa and Suga, 1986), as do auditory neurons in pontine nuclei (Schuller et al., 1991; Kamada et al., 1992) and the cerebellar cortex (Jen and Schlegel, 1980; Jen et al., 1981; Sun et al., 1990) of other bat species.

What acousticomotor responses are influenced by the cerebellar neurons in echolocation? The best evidence relates to the control of vocalization. Thus, ablations of the cerebellar cortex in the mustached bat increase the variabil-

ity of the CF₂ frequency of the sonar pulse (Horikawa and Suga, 1986), which is normally controlled precisely in Doppler shift compensation (Schnitzler, 1970; Henson et al., 1982). This led Horikawa and Suga (1986) to suggest that a major function of auditory cerebellar circuitry is the stabilization of the frequency in sonar pulses. Results from horseshoe bats also implicate pontine neurons in the control of vocalization. Thus, some pontine neurons project directly to motoneurons in nucleus ambiguus that innervate laryngeal muscles controlling vocal frequency (Rübsamen and Schweizer, 1986), and electrical stimulation of the lateral pons in this bat distorts spectral and temporal features of sonar vocalizations (Schuller and Radtke-Schuller, 1990). However, in view of the strength and the broad frequency representation of ICC input to the pons, it is likely that the control of vocalization is only one part of a broader role in controlling acousticomotor responses in echolocation.

Projections to pericollicular areas. Inputs to pericollicular areas vary widely in frequency organization, and may vary correspondingly in their functional roles. For example, the external nucleus of the IC may carry spatial information extracted primarily from 60 kHz echoes. In the present study, it received strong projections only from the 60 kHz region of ICC, consistent with physiological results showing this region to be dominated by sharply tuned 60 kHz neurons (Wenstrup et al., 1986). Most of these neurons display EI response properties (Wenstrup et al., 1986) that could encode azimuthal location (Fuzessery and Pollak, 1985; Wenstrup et al., 1988b). The external nucleus projection to the superior colliculus (Covey et al., 1987) may provide this orientation center with spatial information contained in the 60 kHz component of the bat's echolocation signal.

The area ventral and rostral to ICC, the pericollicular tegmentum, receives projections from the higher ICC frequency bands tested, while input from the fundamental sonar components is uncertain. Like the external nucleus, it appears to project to the superior colliculus (Covey et al., 1987), but its broader frequency composition indicates that it could supply different information to centers involved in spatial orientation. Perhaps it provides spectral information useful to the mustached bat for localizing sounds in elevation (Fuzessery and Pollak, 1985; Fuzessery, 1986).

Central nucleus axons end in two more pericollicular areas, the lateral and medial parts of the nucleus of the brachium of the IC. The lateral part is a group of small, densely packed cells lateral to the brachium (Zook and Casseday, 1982a), with primary ICC input from 60 and 50 kHz representations. Its response properties, other connections, and homologies in nonchiropterans are unknown. The medial part of the nucleus of the brachium comprises a loosely organized cell group placed within and just medial to the brachium, extending from the rostral part of the IC to merge with the medial face of the caudal MGB. This corresponds well to the description of the nucleus in the cat (Berman, 1968; Morest and Oliver, 1984). In the mustached bat, this region receives input from 60 kHz and other frequency bands; this input is noteworthy because some arises from collaterals of tectothalamic axons. The outputs of this nucleus are unknown in the mustached bat, but in cats, the nucleus of the brachium projects to the superior colliculus, the pretectum, and the supragenicular nucleus, among others (Kudo et al., 1984), nuclei involved in spatial orientation and other sensorimotor functions.

Observations on the extrathalamic projections of ICC. By virtue of its strong direct projections to the pontine gray, the external nucleus of the IC, the pericollicular tegmentum, the brachium of the IC, the pretectum, and the supragenicular nucleus of the MGB, the ICC provides significant input to highly interconnected extralemnic pathways involving premotor centers of the superior colliculus, frontal cortex, and cerebellum, to name those currently known. Auditory input to these pathways has been demonstrated in other species. What is unusual in the present results is, first, the degree to which the ICC contributes to information processing within them, and, second, the extent to which ICC outputs remain frequency specific, if not tonotopically organized. These features may reflect the demands of the bat's high speed echolocation behavior, requiring a tight linkage between auditory input and vocal output as well as rapid orienting responses to frequency-specific information contained within distinct components of sonar echoes. The ICC is well situated to provide this information because it integrates and represents, frequency by frequency, input from a host of brain stem auditory nuclei.

Divergent projections of the ICC

The output of the ICC is divergent in several senses. Taken as a whole, this nucleus projects strongly or moderately to at least ten targets (Table 2); this list excludes somewhat weaker projections to the superior colliculus, the contralateral IC, and the auditory brain stem nuclei. Individual frequency-band representations project to many of these regions; in the present study, each provides input to at least six targets. Other studies refine this conclusion, showing that highly restricted parts of an isofrequency representation in ICC project to several nuclei in the MGB and extrathalamic targets (Wenstrup, 1992a).

What remains to be determined, however, are the cellular substrates of this divergence. Do single neurons project broadly to ICC targets, or are they limited to one or a few of these? Several studies have described ICC axons having more than one target. In the cat, for example, some neurons have both brachial and intracollicular branches (Oliver et al., 1991), while several neurons in the rat target both the medial geniculate body and the contralateral inferior colliculus (González-Hernández et al., 1991). In the present study, several axons in the brachium send collaterals both into the nucleus of the brachium and toward the MGB, and a few may project to both supragenicular and ventral nuclei of MGB. Despite this suggestive evidence, the degree of divergence of individual ICC terminations remains obscure, as does the role served by it.

Although the MGB constitutes the most significant target of ICC neurons, these studies nevertheless demonstrate that ICC output is distributed widely throughout the brain of the mustached bat. Although other auditory centers clearly contribute to some of these pathways, the ICC provides strong input to: 1) the primary, tonotopic pathway ascending to auditory cortex; 2) thalamocortical circuits that may be specialized to process information within the mustached bat's biosonar signal; 3) cortical regions that may be involved in vocalization and/or orientation responses; 4) circuits in the superior colliculus and other midbrain regions involved in the reflex orientation to acoustic stimuli or vocalization; and 5) circuitry in the pons and cerebellum that modulates motor activity. Additional circuits are likely to be found as the outputs of ICC targets

are investigated further. Thus, the auditory brain stem input converging onto the IC diverges once again to provide information throughout the neuraxis appropriate for responding to approaching sonar targets or other acoustic signals.

ACKNOWLEDGMENTS

We are grateful to Z.M. Fuzessery for thoughtful comments on the manuscript, to S.L. Pallas for sharing unpublished data with us, and to Ms. Jeanne Popowits and Ms. Carol Grose for their technical assistance. This work was supported by United States Public Health Service grants to J.J.W. (F32 NS07733, R29 DC00937, S07 RR05806) and J.A.W. (R01 DC02319-14).

LITERATURE CITED

- Aas, J.-E. (1989) Subcortical projections to the pontine nuclei in the cat. *J. Comp. Neurol.* 282:331-354.
- Adams, J.C. (1981) Heavy metal intensification of DAB-based HRP reaction product. *J. Histochem. Cytochem.* 29:775.
- Aitkin, L.M., and W.R. Webster (1972) Medial geniculate body of the cat: Organization and responses to tonal stimuli of neurons in ventral division. *J. Neurophysiol.* 35:365-380.
- Andersen, R.A., G.L. Roth, L.M. Aitkin, and M.M. Merzenich (1980) The efferent projections of the central nucleus and the pericentral nucleus of the inferior colliculus in the cat. *J. Comp. Neurol.* 194:649-662.
- Azizi, S.A., R.A. Burne, and D.J. Woodward (1985) The auditory corticopontocerebellar projection in the rat: Inputs to the paraflocculus and midvermis. An anatomical and physiological study. *Exp. Brain Res.* 59:36-49.
- Bateman, G.C., and T.A. Vaughan (1974) Nightly activities of mormoopid bats. *J. Mammal.* 55:45-65.
- Berkley, K.J., and D.C. Mash (1978) Somatic sensory projections to the pretectum in the cat. *Brain Res.* 158:445-449.
- Berman, A.L. (1968) *The Brain Stem of the Cat: A Cytoarchitectonic Atlas With Stereotaxic Coordinates.* Madison: The University of Wisconsin Press.
- Bodenhamer, R.D., and G.D. Pollak (1983) Response characteristics of single units in the inferior colliculus of mustache bats to sinusoidally frequency modulated signals. *J. Comp. Physiol.* 153:67-79.
- Calford, M.B. (1983) The parcellation of the medial geniculate body of the cat defined by the auditory response properties of single units. *J. Neurosci.* 3:2350-2364.
- Calford, M.B., and W.R. Webster (1981) Auditory representation within principal division of cat medial geniculate body: An electrophysiological study. *J. Neurophysiol.* 45:1013-1028.
- Calford, M.B., and L.M. Aitkin (1983) Ascending projections to the medial geniculate body of the cat: Evidence for multiple, parallel auditory pathways through thalamus. *J. Neurosci.* 3:2365-2380.
- Casseday, J.H., J.B. Kobler, S.F. Isbey, and E. Covey (1989) Central acoustic tract in an echolocating bat: An extralemnic auditory pathway to the thalamus. *J. Comp. Neurol.* 287:247-259.
- Clarey, J.C., P. Barone, and T.J. Imig (1992) Physiology of thalamus and cortex. In A.N. Popper and R.R. Fay (eds): *The Mammalian Auditory Pathway: Neurophysiology.* Vol. 2, Springer Handbook of Auditory Research. New York: Springer-Verlag, pp. 232-334.
- Covey, E., W.C. Hall, and J.B. Kobler (1987) Subcortical connections of the superior colliculus in the mustache bat, *Pteronotus parnellii*. *J. Comp. Neurol.* 263:179-197.
- Cowan, W.M., D.I. Gottlieb, A.E. Hendrickson, J.L. Price, and T.A. Woolsey (1972) The autoradiographic demonstration of axonal connections in the central nervous system. *Brain Res.* 37:21-51.
- Edwards, S.T., and A. Hendrickson (1981) The autoradiographic tracing of axonal connections in the central nervous system. In L. Heimer and M.J. RoBards (eds): *Neuroanatomical Tract-Tracing Methods.* New York: Plenum Press, pp. 171-205.
- Frisina, R.D., W.E. O'Neill, and M.L. Zettel (1989) Functional organization of mustached bat inferior colliculus: II. Connections of the FM₂ region. *J. Comp. Neurol.* 284:85-107.
- Fuzessery, Z.M. (1986) Speculations on the role of frequency in sound localization. *Brain Behav. Evol.* 28:95-108.
- Fuzessery, Z.M., and G.D. Pollak (1985) Determinants of sound location selectivity in the bat inferior colliculus: A combined dichotic and free-field stimulation study. *J. Neurophysiol.* 54:757-781.
- Fuzessery, Z.M., J.J. Wenstrup, and G.D. Pollak (1990) Determinants of horizontal sound location selectivity of binaurally excited neurons in an isofrequency region of the mustache bat inferior colliculus. *J. Neurophysiol.* 63:1128-1147.
- Gerfen, C.R., and P.E. Sawchenko (1984) An anterograde neuroanatomical tracing method that shows the detailed morphology of neurons, their axons and terminals: Immunohistochemical localization of an axonally transported plant lectin, *Phaseolus vulgaris* leucoagglutinin (PHA-L). *Brain Res.* 290:219-238.
- González-Hernández, T.H., D. Galindo-Mireles, A. Castañeyra-Perdomo, and R. Ferrer-Torres (1991) Divergent projections of projecting neurons of the inferior colliculus to the medial geniculate body and the contralateral inferior colliculus in the rat. *Hearing Res.* 52:17-22.
- Hashikawa, T. (1983) The inferior colliculopontine neurons of the cat in relation to other collicular descending neurons. *J. Comp. Neurol.* 219:241-249.
- Henson, O.W., G.D. Pollak, J.B. Kobler, M.M. Henson, and L.J. Goldman (1982) Cochlear microphonic potentials elicited by biosonar signals in flying bats, *Pteronotus p. parnellii*. *Hearing Res.* 7:127-147.
- Horikawa, J., and N. Suga (1986) Biosonar signals and cerebellar auditory neurons of the mustached bat. *J. Neurophys.* 55:1247-1267.
- Imig, T.J., and A. Morel (1985) Tonotopic organization in ventral nucleus of medial geniculate body in the cat. *J. Neurophysiol.* 53:309-340.
- Izzo, P.N. (1991) A note on the use of biocytin in anterograde tracing studies in the central nervous system: Application at both light and electron microscopic level. *J. Neurosci. Methods* 36:155-166.
- Jen, P.H.-S., and P.A. Schlegel (1980) Neurons in the cerebellum of echolocating bats respond to acoustic signals. *Brain Res.* 196:502-507.
- Jen, P.H.-S., M. Vater, G. Harnischfeger, and R. Rübsamen (1981) Mapping of the auditory area in the cerebellar vermis and hemispheres of the little brown bat, *Myotis lucifugus*. *Brain Res.* 219:156-161.
- Jen, P.H.-S., X.M. Sun, and T. Kamada (1982) Responses of cerebellar neurons of the CF-FM bat, *Pteronotus parnellii* to acoustic stimuli. *Brain Res.* 252:167-171.
- Jones, E.G., and A.J. Rockel (1971) The synaptic organization in the medial geniculate body of afferent fibres ascending from the inferior colliculus. *Z. Zellforsch. Mikrosk. Anat.* 113:44-66.
- Kamada, T., M. Wu, and P.H.-S. Jen (1992) Auditory response properties and spatial response areas of single neurons in the pontine nuclei of the big brown bat, *Eptesicus fuscus*. *Brain Res.* 575:187-198.
- Kawamura, K., and M. Chiba (1979) Cortical neurons projecting to the pontine nuclei in the cat. An experimental study with the horseradish peroxidase technique. *Exp. Brain Res.* 35:269-285.
- King, M.A., P.M. Louis, B.E. Hunter, and D.W. Walker (1989) Biocytin: A versatile anterograde neuroanatomical tract-tracing alternative. *Brain Res.* 497:361-367.
- Kobler, J.B., S.F. Isbey, and J.H. Casseday (1987) Auditory pathways to the frontal cortex of the mustache bat, *Pteronotus parnellii*. *Science* 236:824-826.
- Kössl, M., and M. Vater (1985) The cochlear frequency map of the mustache bat, *Pteronotus parnellii*. *J. Comp. Physiol. A* 157:687-697.
- Kudo, M., and K. Niimi (1978) Ascending projections of the inferior colliculus onto the medial geniculate body in the cat studied by anterograde and retrograde tracing techniques. *Brain Res.* 155:113-117.
- Kudo, M., and K. Niimi (1980) Ascending projections of the inferior colliculus in the cat: An autoradiographic study. *J. Comp. Neurol.* 191:545-556.
- Kudo, M., K. Itoh, S. Kawamura, and N. Mizuno (1983) Direct projections to the pretectum and the midbrain reticular formation from auditory relay nuclei in the lower brainstem of the cat. *Brain Res.* 288:13-19.
- Kudo, M., T. Tashiro, S. Higo, T. Matsuyama, and S. Kawamura (1984) Ascending projections from the nucleus of the brachium of the inferior colliculus in the cat. *Exp. Brain Res.* 54:203-211.
- Kurokawa, T., K. Yoshida, T. Yamamoto, and H. Oka (1990) Frontal cortical projections from the supragenicular nucleus in the rat, as demonstrated by the PHA-L method. *Neurosci. Lett.* 120:259-262.
- LeDoux, J.E., D.A. Ruggiero, and D.J. Reis (1985) Projections to the subcortical forebrain from anatomically defined regions of the medial geniculate body in the rat. *J. Comp. Neurol.* 242:182-213.
- LeDoux, J.E., A. Sakaguchi, J. Iwata, and D.J. Reis (1986) Interruption of projections from the medial geniculate body to an archi-neostriatal field

- disrupts the classical conditioning of emotional responses to acoustic stimuli. *Neuroscience* 17:615-627.
- Lesser, H.D. (1988) Encoding of Amplitude-Modulated Sounds by Single Units in the Inferior Colliculus of the Mustached Bat, *Pteronotus parnellii*. Doctoral dissertation: University of Rochester, Rochester, NY, pp. 1-203.
- Lesser, H.D., W.E. O'Neill, R.D. Frisina, and R.C. Emerson (1990) ON-OFF units in the mustached bat inferior colliculus are selective for transients resembling "acoustic glint" from fluttering insect targets. *Exp. Brain Res.* 82:137-148.
- Lieberman, M.C. (1991) Central projections of auditory-nerve fibers of differing spontaneous rate. I. Anteroventral cochlear nucleus. *J. Comp. Neurol.* 313:240-258.
- Majorossy, K., and M. Réthelyi (1968) Synaptic architecture in the medial geniculate body (ventral division). *Exp. Brain Res.* 6:306-323.
- Majorossy, K., and A. Kiss (1976) Specific patterns of neuron arrangement and of synaptic articulation in the medial geniculate body. *Exp. Brain Res.* 26:1-17.
- Mesulam, M.-M. (1982) Principles of horseradish peroxidase neurohistochemistry and their applications for tracing neural pathways—axonal transport, enzyme histochemistry and light microscopic analysis. In M.-M. Mesulam (ed): *Tracing Neural Connections with Horseradish Peroxidase*. Chichester: John Wiley & Sons, pp. 1-151.
- Middlebrooks, J.C., and J.M. Zook (1983) Intrinsic organization of the cat's medial geniculate body identified by projections to binaural response-specific bands in the primary auditory cortex. *J. Neurosci.* 3:203-224.
- Mihailoff, G.A., R.J. Kosinski, S.A. Azizi, and B.G. Border (1989) Survey of noncortical afferent projections to the basilar pontine nuclei: A retrograde tracing study in the rat. *J. Comp. Neurol.* 282:617-643.
- Moore, J.K., F. Karapas, and R.Y. Moore (1977) Projections of the inferior colliculus in insectivores and primates. *Brain Behav. Evol.* 14:301-327.
- Morest, D.K. (1964) The neuronal architecture of the medial geniculate body of the cat. *J. Anat. (Lond.)* 98:611-630.
- Morest, D.K. (1965) The laminar structure of the medial geniculate body of the cat. *J. Anat. (Lond.)* 99:143-160.
- Morest, D.K., and D.L. Oliver (1984) The neuronal architecture of the inferior colliculus in the cat: Defining the functional anatomy of the auditory midbrain. *J. Comp. Neurol.* 222:209-236.
- Novick, A. (1963) Orientation in neotropical bats. II. Phyllostomatidae and Desmodontidae. *J. Mammal.* 44:44-56.
- Oliver, D.L., and W.C. Hall (1978) The medial geniculate body of the tree shrew, *Tupaia glis*. I. Cytoarchitecture and midbrain connections. *J. Comp. Neurol.* 182:423-458.
- Oliver, D.L., S. Kuwada, T.C.T. Yin, L.B. Haberly, and C.K. Henkel (1991) Dendritic and axonal morphology of HRP-injected neurons in the inferior colliculus of the cat. *J. Comp. Neurol.* 303:75-100.
- Olsen, J.F. (1986) Processing of Biosonar Information by the Medial Geniculate Body of the Mustached Bat, *Pteronotus parnellii*. Doctoral dissertation: Washington University, St. Louis, MO, pp. 1-325.
- Olsen, J.F., and N. Suga (1991a) Combination-sensitive neurons in the medial geniculate body of the mustached bat: Encoding of relative velocity information. *J. Neurophysiol.* 65:1254-1274.
- Olsen, J.F., and N. Suga (1991b) Combination-sensitive neurons in the medial geniculate body of the mustached bat: Encoding of target range information. *J. Neurophysiol.* 65:1275-1296.
- O'Neill, W.E. (1985) Responses to pure tones and linear FM components of the CF-FM biosonar signal by single units in the inferior colliculus of the mustached bat. *J. Comp. Physiol. A* 157:797-815.
- O'Neill, W.E., and N. Suga (1982) Encoding of target range and its representation in the auditory cortex of the mustached bat. *J. Neurosci.* 2:17-31.
- O'Neill, W.E., R.D. Frisina, and D.M. Gooler (1989) Functional organization of mustached bat inferior colliculus: I. Representation of FM frequency bands important for target ranging revealed by 14C-2-deoxyglucose autoradiography and single unit mapping. *J. Comp. Neurol.* 284:60-84.
- Pallas, S.L., J. Hahm, and M. Sur (1991) Axonal arborizations in the medial geniculate nucleus of ferrets: Comparison of arbors from the inferior colliculus with induced inputs from retinal ganglion cells. *Proc. Soc. Neurosci.* 17:304 (abstract).
- Pollak, G.D., and R.D. Bodenhamer (1981) Specialized characteristics of single units in inferior colliculus of mustache bat: Frequency representation, tuning, and discharge patterns. *J. Neurophysiol.* 46:605-620.
- Rainey, W.T., and E.G. Jones (1983) Spatial distribution of individual medial lemniscal axons in the thalamic ventrobasal complex of the cat. *Exp. Brain Res.* 49:229-246.
- Riquimaroux, H., S.J. Gaioni, and N. Suga (1991) Cortical computational maps control auditory perception. *Science* 251:565-568.
- Rodrigues-Dagauff, C., G. Simm, Y. de Ribaupierre, A. Villa, F. de Ribaupierre, and E. Rouiller (1989) Functional organization of the ventral division of the medial geniculate body of the cat: Evidence for a rostro-caudal gradient of response properties and cortical projections. *Hearing Res.* 39:103-126.
- Rose, J.E., and C.N. Woolsey (1949) The relations of thalamic connections, cellular structure and evocable electrical activity in the auditory region of the cat. *J. Comp. Neurol.* 91:441-466.
- Ross, L.S., G.D. Pollak, and J.M. Zook (1988) Origin of ascending projections to an isofrequency region of the mustache bat's inferior colliculus. *J. Comp. Neurol.* 270:488-505.
- Rouiller, E.M., and F. de Ribaupierre (1985) Origin of afferents to physiologically defined regions of the medial geniculate body of the cat: Ventral and dorsal divisions. *Hearing Res.* 19:97-114.
- Rouiller, E., Y. de Ribaupierre, and F. de Ribaupierre (1979) Phase-locked responses to low frequency tones in the medial geniculate body. *Hearing Res.* 1:213-226.
- Rouiller, E.M., R. Cronin-Schreiber, D.M. Fekete, and D.K. Ryugo (1986) The central projections of intracellularly labeled auditory nerve fibers in cats: An analysis of terminal morphology. *J. Comp. Neurol.* 249:261-278.
- Rübsamen, R., and H. Schweizer (1986) Control of echolocation pulses by neurons of the nucleus ambiguus in the rufous horseshoe bat, *Rhinolophus rouxi*. *J. Comp. Physiol. A* 159:689-699.
- Ryugo, D.K., and E.M. Rouiller (1988) Central projections of intracellularly labeled auditory nerve fibers in cats: Morphometric correlations with physiological properties. *J. Comp. Neurol.* 271:130-142.
- Ryugo, D.K., and S. Sento (1991) Synaptic connections of the auditory nerve in cats: Relationship between endbulbs of held and spherical bushy cells. *J. Comp. Neurol.* 305:35-48.
- Saldaña, E., and M.A. Merchán (1992) Intrinsic and commissural connections of the rat inferior colliculus. *J. Comp. Neurol.* 319:417-437.
- Schnitzler, H.-U. (1970) Echoortung bei der Fledermaus *Chilonycteris rubiginosa*. *Z. Vergl. Physiol.* 68:25-38.
- Schuller, G., and S. Radtke-Schuller (1990) Neural control of vocalization in bats: Mapping of brainstem areas with electrical microstimulation eliciting species-specific echolocation calls in the rufous horseshoe bat. *Exp. Brain Res.* 79:192-206.
- Schuller, G., E. Covey, and J.H. Casseday (1991) Auditory pontine grey: Connections and response properties in the horseshoe bat. *Eur. J. Neurosci.* 3:648-662.
- Schweizer, H. (1981) The connections of the inferior colliculus and the organization of the brainstem auditory system in the greater horseshoe bat (*Rhinolophus ferrumequinum*). *J. Comp. Neurol.* 201:25-49.
- Smith, P.H., and W.S. Rhode (1987) Characterization of HRP-labeled globular bushy cells in the cat anteroventral cochlear nucleus. *J. Comp. Neurol.* 266:360-375.
- Suga, N. (1984) The extent to which biosonar information is represented in the bat auditory cortex. In G.M. Edelman, W.E. Gall, and W.M. Cowan (eds): *Dynamic Aspects of Neocortical Function*. New York: John Wiley & Sons, pp. 315-373.
- Suga, N., and P.H.-S. Jen (1976) Disproportionate tonotopic representation for processing CF-FM sonar signals in the mustache bat auditory cortex. *Science* 194:542-544.
- Suga, N., and J. Horikawa (1986) Multiple time axes for representation of echo delays in the auditory cortex of the mustached bat. *J. Neurophysiol.* 55:776-805.
- Suga, N., W.E. O'Neill, K. Kujirai, and T. Manabe (1983) Specificity of combination-sensitive neurons for processing of complex biosonar signals in auditory cortex of the mustached bat. *J. Neurophysiol.* 49:1573-1626.
- Sun, D., X. Sun, and P.H.-S. Jen (1990) The influence of the auditory cortex on acoustically evoked cerebellar responses in the CF-FM bat, *Rhinolophus pearsoni chinensis*. *J. Comp. Physiol. A* 166:477-487.
- Wenstrup, J.J. (1990) Strong projection to the pontine gray from the inferior colliculus of the mustached bat. *Proc. Soc. Neurosci.* 16:717 (abstract).
- Wenstrup, J.J. (1992a) Monaural and binaural regions of the mustached bat's inferior colliculus project differently to targets in the medial geniculate body and pons. *Assoc. Res. Otolaryngol.* 16:77 (abstract).
- Wenstrup, J.J. (1992b) Inferior colliculus projections to the medial geniculate body: A study of the anatomical basis of combination-sensitive neurons in the mustached bat. *Proc. Soc. Neurosci.* 18:1039 (abstract).

- Wenstrup, J.J., L.S. Ross, and G.D. Pollak (1986) Binaural response organization within a frequency-band representation of the inferior colliculus: Implications for sound localization. *J. Neurosci.* 6:962-973.
- Wenstrup, J.J., Z.M. Fuzessery, and G.D. Pollak (1988a) Binaural neurons in the mustache bat's inferior colliculus. I. Responses of 60-kHz EI units to dichotic sound stimulation. *J. Neurophysiol.* 60:1369-1383.
- Wenstrup, J.J., Z.M. Fuzessery, and G.D. Pollak (1988b) Binaural neurons in the mustache bat's inferior colliculus. II. Determinants of spatial responses of 60-kHz EI units. *J. Neurophysiol.* 60:1384-1404.
- Wiberg, M., J. Westman, and A. Blomqvist (1986) The projection to the mesencephalon from the sensory trigeminal nuclei. An anatomical study in the cat. *Brain Res.* 399:51-68.
- Winer, J.A. (1985) The medial geniculate body of the cat. *Adv. Anat. Embryol. Cell Biol.* 86:1-98.
- Winer, J.A. (1991) Anatomy of the medial geniculate body. In R.A. Altschuler, R.P. Bobbin, B.M. Clopton, and D.W. Hoffman (eds): *Neurobiology of Hearing: The Central Auditory System*. New York: Raven Press, pp. 293-333.
- Winer, J.A. (1992) The functional architecture of the medial geniculate body and the primary auditory cortex. In D.B. Webster, A.N. Popper, and R.R. Fay (eds): *The Mammalian Auditory Pathway: Neuroanatomy*. Vol. 1, Springer Handbook of Auditory Research. New York: Springer-Verlag, pp. 222-409.
- Winer, J.A., and D.K. Morest (1984) Axons of the dorsal division of the medial geniculate body of the cat: A study with the rapid Golgi method. *J. Comp. Neurol.* 224:344-370.
- Winer, J.A., and J.J. Wenstrup (1994a) Cytoarchitecture of the medial geniculate body in the mustached bat. *J. Comp. Neurol.* 346:161-182.
- Winer, J.A., and J.J. Wenstrup (1994b) The neurons of the medial geniculate body in the mustached bat (*Pteronotus parnellii*). *J. Comp. Neurol.* 346:183-206.
- Winer, J.A., J.J. Wenstrup, and D.T. Larue (1992) Patterns of GABAergic immunoreactivity define subdivisions of the mustached bat's medial geniculate body. *J. Comp. Neurol.* 319:172-190.
- Wu, S.H., and D. Oertel (1984) Intracellular injection with horseradish peroxidase of physiologically characterized stellate and bushy cells in slices of mouse anteroventral cochlear nuclei. *J. Neurosci.* 4:1577-1588.
- Yoshida, A., B.J. Sessle, J.O. Dostrovsky, and C.Y. Chiang (1992) Trigeminal and dorsal column nuclei projections to the anterior pretectal nucleus in the rat. *Brain Res.* 590:81-94.
- Zook, J.M., and J.H. Casseday (1982a) Cytoarchitecture of auditory system in lower brainstem of the mustache bat, *Pteronotus parnellii*. *J. Comp. Neurol.* 207:1-13.
- Zook, J.M., and J.H. Casseday (1982b) Origin of ascending projections to inferior colliculus in the mustache bat, *Pteronotus parnellii*. *J. Comp. Neurol.* 207:14-28.
- Zook, J.M., and J.H. Casseday (1987) Convergence of ascending pathways at the inferior colliculus of the mustache bat, *Pteronotus parnellii*. *J. Comp. Neurol.* 261:347-361.
- Zook, J.M., and P.A. Leake (1989) Connections and frequency representation in the auditory brainstem of the mustache bat, *Pteronotus parnellii*. *J. Comp. Neurol.* 290:243-261.
- Zook, J.M., J.A. Winer, G.D. Pollak, and R.D. Bodenhamer (1985) Topology of the central nucleus of the mustache bat's inferior colliculus: Correlation of single unit response properties and neuronal architecture. *J. Comp. Neurol.* 231:530-546.